Heliyon 10 (2024) e39901

Contents lists available at ScienceDirect

Heliyon

journal homepage: www.cell.com/heliyon

Research article

Comprehensive analysis of faults and diagnosis techniques in cascaded multi-level inverters

Ranjith Kumar Gatla [a], Devineni Gireesh Kumar [b], Palthur Shashavali [c], Rao Dsnm [d], Hossam Kotb [e], Abdulaziz Alkuhayli [f], Yazeed Yasin Ghadi [g], Wulfran Fendzi Mbasso [h,*]

[a] Department of Electrical & Electronics Engineering, Institute of Aeronautical Engineering, Dundigal, Telangana, 500043, India
[b] Department of Electrical & Electronics Engineering, B V Raju Institute of Technology, Narsapur, Telangana, 502313, India
[c] Department of EEE, S K University College of Engineering & Technology, Ananthapuramu, Andhra Pradesh, 515003, India
[d] Department of EEE, Gokaraju Rangaraju Institute of Engineering & Technology, Bachupally, 500090, Telangana, India
[e] Department of Electrical Power and Machines, Faculty of Engineering, Alexandria University, Alexandria 21544, Egypt
[f] Electrical Engineering Department, College of Engineering, King Saud University, Riyadh 11421, Saudi Arabia
[g] Department of Computer Science and Software Engineering, Al Ain University, Abu Dhabi 15322, United Arab Emirates
[h] Laboratory of Technology and Applied Sciences, University Institute of Technology, University of Douala, PO Box: 8698, Douala, Cameroon

ARTICLE INFO

Keywords:
Multi-level inverters
Fault detection
Total harmonic distortion
Open-loop and closed-loop systems

ABSTRACT

Reliability is a crucial factor to consider for multi-level inverters (MLIs) used in industrial applications. With the increasing number of power semiconductor devices, the potential for defects to significantly degrade the overall system is heightened. A highly effective fault-detection technique is required to minimize the impact of faults. This paper provides a comprehensive overview of the fundamental principles of multi-level inverters and the various sorts of faults that can occur in multi-level inverters. This study provides a comprehensive analysis of five-level cascaded H-bridge multilevel inverters (MLIs) under both normal and defective conditions. The paper outlines a fault-detection method that utilizes total harmonic distortion and a normalized output voltage factor. In addition, the paper discusses a fault-isolation strategy that relies on reducing amplitude modulation. This method leads to the development of a fault-tolerant inverter. The utilization of level-shifted pulse-width modulation (LSPWM) technology is employed for the purpose of switching operations. LSPWM is the most appropriate technique for MLIs that require a low amount of computational resources. The fault-diagnosis approach given is suitable for MLI-based drives, grid-connected operations, and other applications. This paper presents a comprehensive examination of the 5L-CMLI (5-Level Cascaded Multi-Level Inverter) under various fault scenarios in CMLI. Subsequently, various fault diagnosis approaches will be examined, including their advantages and disadvantages. The paper discusses several defects that can occur in the Insulated Gate Bipolar Transistor (IGBT) of a Current Mode Logic Inverter (CMLI), and also presents a design for a reliable fault diagnosis system. Furthermore, this analysis examines several fault detection strategies in CMLI, categorized according to open-loop and closed-loop dynamic systems fault classifications.

* Corresponding author.
E-mail addresses: ranjith.gatla@gmail.com (R.K. Gatla), gireesh218@gmail.com (D.G. Kumar), shashavali240@gmail.com (P. Shashavali), dsnm.rao@gmail.com (R. Dsnm), hossam.kotb@alexu.edu.eg (H. Kotb), aalkuhayli@ksu.edu.sa (A. Alkuhayli), yazeed.ghadi@aau.ac.ae (Y.Y. Ghadi), fendzi.wulfran@yahoo.fr (W.F. Mbasso).

https://doi.org/10.1016/j.heliyon.2024.e39901
Received 8 April 2024; Received in revised form 21 October 2024; Accepted 25 October 2024
Available online 28 October 2024

1. Introduction

Multi-level inverter (MLI) topologies have emerged as one of the most prominent fields of power electronics research within the last ten years. This is due to intelligent MLI technology's intrinsic capacity to provide output with lower total harmonic distortion (THD), lower electromagnetic interference, high power quality, and smaller filters [1,2]. It may also synthesize the waveform in a staircase way. Because of these benefits, MLIs are employed in many different applications, including flexible AC gearbox systems, active filters, renewable energy systems, and electrical motor drives [3–5]. Three fundamental topologies of MLIs are distinguished: neutral point clamped (NPC) [6], flying capacitor (FC) [7,8] and cascaded H-bridge (CHB) [9]. In order to address specific drawbacks, other topologies have been developed from these fundamental topologies, such as active neutral point clamping [10–12], modular multi-level converter (MMC) [13] and the multi-level DC link inverter [14]. The number of the employed switching semiconductor devices determines how reliable power electronics converters are. Better output voltage quality is provided by the MLI at the expense of more static semiconductor devices. MLI dependability is, therefore, a very important problem. Multiple power semiconductor devices are switched, which increases the possibility of numerous errors occurring and decreases device dependability. Two-thirds of faults found in power semiconductor devices and 13 % in soldiers were found in surveys and research conducted on more than 200 industrial processes and 80 organizations. The failure of the device module accounts for 34 % of all converter malfunctions [15]. Apart from the diverse reasons for malfunctions, power semiconductor switch malfunctions may be classified into two primary categories: open-circuit switch faults (OCSFs) and short-circuit switch faults (SCSFs).

Numerous research articles have documented the identification of faults in power semiconductor apparatus. In Ref. [16], the fault-diagnostic technique employing average current Park's vector (ACPV) for three-level NPC MLIs is presented. The normalized average value of motor line current in the ACPV algorithm indicates the problematic switch, while ACPV itself identifies the damaged switch leg. A three-level NPC fault-detection method based on output pole voltage and current is discussed in Ref. [17]. The discrepancies between normalized output voltages and the corresponding control switching states are exploited by this approach. To locate the short circuit issue in FC MLIs, a vector-based diagnostic and output voltage frequency analysis are used [18,19]. In Ref. [20], a model-based predictive control method for switch fault identification is provided. In Ref. [21], an asymmetric zero voltage state-based open-circuit fault-diagnosis method for CHB MLIs is reported. A simpler approach based on zero voltage switching has been provided by the authors and verified for both linear and nonlinear loads. For five-level CHB MLIs, the authors of [22] have provided a short circuit identification technique based on the comparison of output voltage with reference voltage. In Ref. [23], a neural network-based technique for defect diagnosis for five-level CHB MLIs is put forward. The kind and location of the defect are determined using five multilayer perception networks. A straightforward THD-based fault-diagnosis method for five-level CHB MLIs has been provided by the authors of [24]. The normalized pole output current is used to identify the likely malfunctioning switch. In Ref. [25], a knowledge-based model and state observer for failure detection and reconfiguration method for MMCs are presented.

Multi-Level Inverters (MLIs) have emerged as a prominent technology in power electronics due to their superior performance in terms of output voltage quality, reduced harmonics, and enhanced efficiency. However, the complexity of MLI topologies and the increasing number of switching devices can lead to various fault conditions, such as open-circuit switch faults (OCSFs) and short-circuit switch faults (SCSFs), which can significantly degrade system performance and reliability. To prevent numerous switch faults that might shut down a whole operation, post-fault control is required. Actually, after fault diagnosis, a post-fault control scheme needs to be implemented for a fully fault-tolerant operation. The post-fault control method attracts researchers' interest. The widely used techniques of fundamental phase-shift compensation (FPSC) and avoiding malfunctioning operational cells are described in Refs. [26–29]. To avoid the flawed cell algorithm and achieve balanced three-phase functioning, an equal number of cells are eliminated. In FPSC, the phase shift of the fundamental wave of all three phases will alter to maintain a balanced operation; however, in this approach, the load voltage is decreased to 40 % of its healthy condition value. The voltage drop is limited to 23 % of the healthy level. Nonetheless, the power factor can be impacted. In order to overcome the defect, a space vector-based control technique is adopted in Refs. [30–32], along with redundant switching states. This paper presents an open-circuit fault-detection method for five-level CHB MLIs. A detailed examination of output voltage fluctuation and THD in both healthy and malfunctioning CHB MLIs is given. The suggested fault-diagnosis method may be used with almost any MLI based on industrial applications. In addition, the method is highly economical and may be used with few adjustments in current systems. The method under investigation is predicated on a normalized output voltage factor and THD measurement. One to two fundamental periods can be used to identify a potential open-circuit switch problem based on the threshold calculations. Any power electronics MLI system based on closed-loop operation already contains one voltage sensor per phase, which is all that is needed for the fault-diagnosis approach that has been described. Sivapriya and Kalaiarasi (2023) presented a unique improved deep learning-based defect diagnostic technique in their research that was published in e-Prime. This investigation was published in 2023. They underline the significance of using deep learning models in order to improve the accuracy of defect detection and the reaction time in MLIs [33]. A number of different approaches to training neural networks are described in this paper. The purpose of the study is to enhance diagnostic skills in situations with complicated faults.

In a different piece of research, Sivapriya and colleagues (2023) used a multiscale kernel convolutional neural network, also known as an MK-CNN, to identify problem areas in cascaded MLIs. This method is able to successfully extract features from time-series data, which results in an increase in the rate of fault identification [34]. Through the use of convolutional layers, the model is able to recognize small irregularities that conventional approaches could miss. An intelligent diagnostic method was presented by Du et al. (2023), which is a combination of deep convolutional neural networks and sparse representation. In order to improve the capability of reliably diagnosing defects in H-bridge cascaded MLIs, this new solution takes use of the characteristics that both methodologies provide. When compared to more traditional methods, the authors showed that the use of a hybrid model resulted in considerable gains in detection efficiency [35].

Artificial neural networks (ANNs) were investigated by Raj et al. (2018) for the purpose of fault detection in asymmetric multilevel inverters. This study exemplifies the adaptability of machine learning methodologies, since it demonstrates the ability to identify faults in asymmetric inverters [36]. In diagnostic procedures, their results indicate that artificial neural networks (ANNs) have the potential to properly diagnose problems and minimize reaction times. The authors Wang et al. (2016) developed a technique for defect detection that was based on support vector machines (SVM), the fast Fourier transform (FFT), and the robust principal component analysis (RPCA) [37]. A considerable improvement in defect detection accuracy is achieved with the use of both frequency domain and statistical approaches, as shown by this integrated methodology. An improved support vector machine approach that was augmented by a gray wolf optimization algorithm was suggested by Yuan et al. (2023) for the purpose of detecting faults in H-bridge cascaded five-level inverters [38]. According to the results of their investigation, improving the settings of the support vector machine (SVM) using the gray wolf algorithm results in improved generalization over a wide range of operating situations and a greater level of accuracy in defect identification. Ali and colleagues (2021) conducted a study to investigate the utilization of machine learning techniques for the purpose of identifying open switch faults in cascade H-bridge multi-level inverters that are used in distributed power producers [39]. The research demonstrates that machine learning is an excellent method for tackling real-time fault diagnostic difficulties, and it also highlights the usefulness of this method in practical contexts.

An innovative approach to diagnostic strategies was presented by Rinsha and Jagadanand (2023), who presented a rolling average-decision tree-based technique for fault identification in neutral point-clamped inverters [40]. This method offers a unique viewpoint on diagnostic methods. The work that they have done highlights the need of developing adaptable approaches that are able to handle a wide range of operating settings and fault kinds. For the purpose of fault identification in multi-level inverters, Parimalasundar et al. (2024) introduced an innovative technique that makes use of artificial neural networks [41]. When it comes to improving the dependability and performance of MLIs, this research makes a contribution to the expanding body of evidence that supports the usefulness of artificial neural networks (ANNs).

Existing research has explored various fault detection methods for MLIs, including those based on average current Park's vector, output pole voltage and current, vector-based diagnosis, model-based predictive control, and neural networks. While these methods have shown promise, they often suffer from limitations such as sensitivity to noise, computational complexity, or the requirement for specific operating conditions.

Despite the advancements in fault detection for MLIs, there remains a significant research gap in developing robust and efficient methods that can accurately detect and diagnose faults under various operating conditions, especially in the presence of noise and disturbances. Additionally, the integration of fault detection with post-fault control strategies to ensure continuous system operation is an area that requires further investigation. This paper aims to address the aforementioned research gap by presenting a comprehensive review of the existing literature on MLI fault detection and post-fault control. This comprehensive review of the existing literature on MLI fault detection and control, critically evaluating state-of-the-art techniques, identifying their limitations, and highlighting the key challenges that hinder their effectiveness. Moreover, proposed promising research directions and future perspectives for the development of innovative fault detection and control methods that address these challenges and enhance the reliability and performance of MLI systems.

2. Basic of inverters

2.1. Conventional inverters

An inverter is a device that converts from a DC supply to an AC supply. It is called a power inverter. It comprises solid-state switches like BJT, MOSFET, IGBT, Thyristors, etc., and loss-less components such as inductors and capacitors. The basic block diagram of the inverter is shown in Fig. 1. Table 1 represents the types of electrical power with variable properties during the conversion.

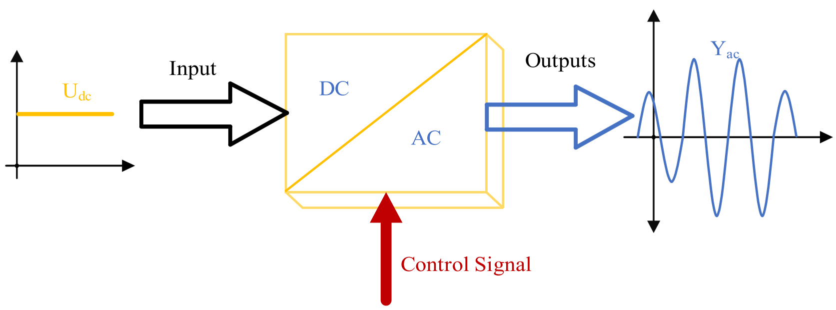

Fig. 1. Basic diagram of the inverter.

Table 1
Conversion of electric power.

Types of electric power	Changeable properties
Direct Current	Magnitude
Alternating Current	Magnitude, Frequency, No. of phases

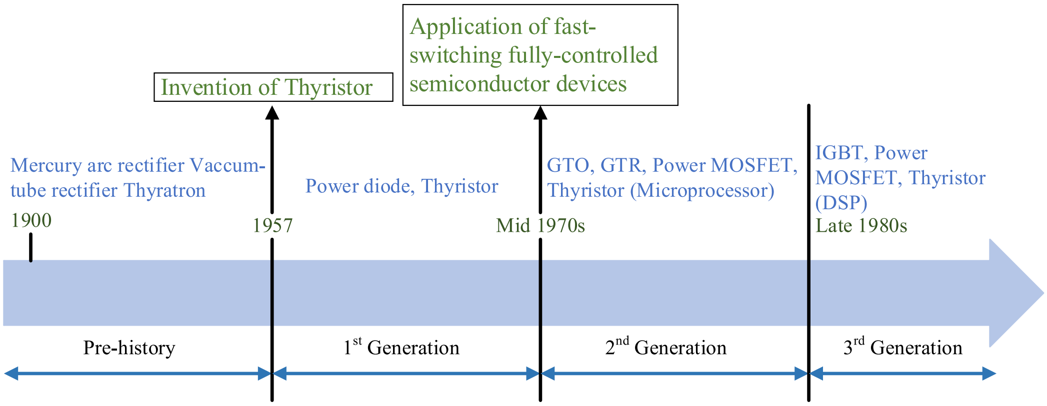

Fig. 2. History of power electronic switches.

Drawbacks of two-level Inverters.

- 10,000 V/μs is the highest $\frac{dv}{dt}$ inverter output voltage value.
- Motor harmonic losses.

These can be solved with the proper addition of a tuned LC filter. So, the cost will be increased.

In early 90's, research on power electronics switches started. In 1957, Thyristor was invented. In the mid 1970's, GTO, GTR, Power MOSFET, Thyristor are came into existence. In late 1980's, IGBT, Power MOSFET and DSP were invented. The history of power electronics switches are shown in Fig. 2.

2.2. Multi-level inverters

MLI's are used for industrial purposes in high power applications and renewable energy sources. Many researchers are paying worthwhile attention to multi-level inverter topologies from the past several years and still significant research is preceding towards the development of new multi-level inverter topologies. In conventional power inverters, output attains high harmonic distortions and high dv/dt.

MLI offsets these drawbacks to the conventional power Inverters. As the level of the Inverter increases, the output dv/dt decreases. The power and voltage ratings are shown in Fig. 3.

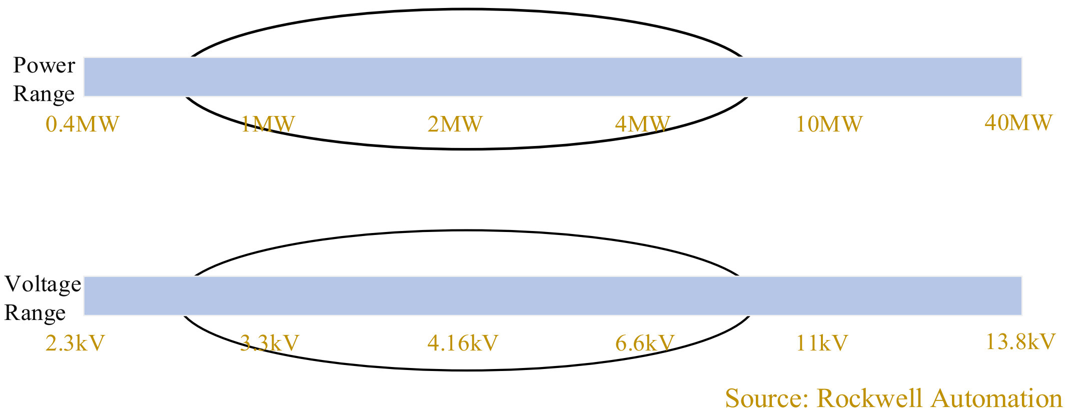

Fig. 3. Medium voltage drives.

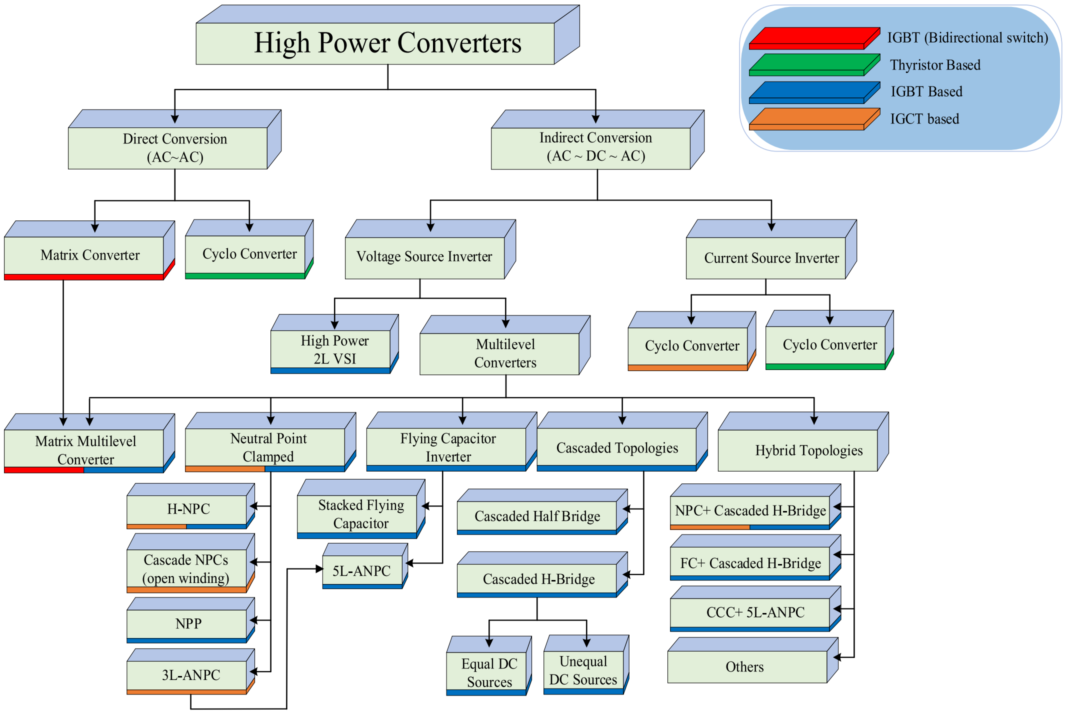

Fig. 4. Classifications of inverters.

2.2.1. *Classifications of MLI*

MLI is the preferred choice for many industrial applications and academia. MLI's are used for commercial purposes in many applications such as grinders, compressors, mills, conveyors, pumps, compensators, HVDC conversions and so on. Many researchers are paying great attention to get better improvement in reliability, high efficiency and cost effective with multiple topologies. Three main classifications of MLI are given below. Detailed classification of inverters is shown in Fig. 4.

a) Diode Clamped MLI (NPC MLI)
b) Flying Capacitor MLI (FC MLI)
c) Cascaded H-Bridge MLI (CMLI)
a) Diode Clamped MLI (NPC MLI)

In 1981, Nabe et al. proposed a neutral point-clamped inverter. In the decade of the 90s, researchers published many articles on different levels of NPC inverters and suggested the utilization of NPC inverters in applications such as variable drives, SVC, high-power applications, etc. A five-level single-phase NPC inverter is shown in Fig. 5. In a single phase, the level of the NPC inverter includes four capacitors; therefore, these four capacitors charging levels are up to source voltage *E*. Clamping diodes clamp the voltage stress across each switch to *E*. Table 2 generates the output voltage levels for where V_o, i.e., dc voltage used as a reference. For instance, four complimentary switches are used in each phase. (T_1, T_1'), (T_2, T_2'), (T_3, T_3'), (T_4, T_4') pair are switches. The switch will be 'ON' if the state condition is '1' and 'OFF' if the state condition is '0'. It is obvious that the '*k*' level NPC Inverter has (*2k-1*) output level output voltage if four switches are 'ON' in any position at any given time.

b) Flying Capacitor MLI (FC MLI)

In 1992, Meynord et al. proposed flying capacitor inverter. The FC inverter design was similar to NPC Inverter. It used FC instead of clamped diodes. Fig. 6 shows the five-level single phase FC inverter. FC inverters have ladder structure with dc side capacitors. Capacitor voltage differs from capacitor to capacitor. Voltage increment in between adjacent capacitors has responsibility of the output voltage levels.

In FC inverter output voltage can be synthesized with two or more valid switches by which, it has redundancies in inner voltages. Table 3 shows the output stages. FC inverter doesn't require all switches in same conduction like NPC Inverters. NPC inverter has line-line redundancies while FC inverter has phase redundancies. FC inverter $\langle k-1\rangle$ dc side capacitor is required with additionally $(\langle k-1\rangle * \langle k-2\rangle)/2)$ auxiliary capacitor for each leg.

c) Cascaded H-Bridge MLI (CMLI)

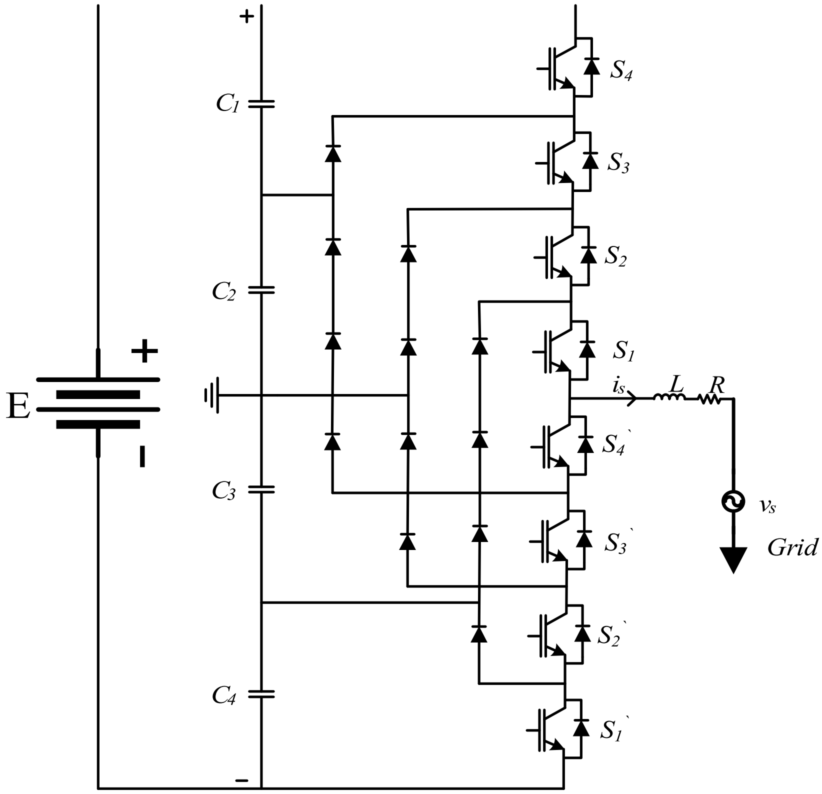

Fig. 5. Single phase 5L-NPC inverter.

Table 2
Diode clamped 5-level switching states.

Output Voltage(V)	Switching States							
	T_4	T_3	T_2	T_1	T_4`	T_3`	T_2`	T_1`
$V_4 = 4E$	ON	ON	ON	ON	OFF	OFF	OFF	OFF
$V_3 = 3E$	OFF	ON	ON	ON	ON	OFF	OFF	OFF
$V_2 = 2E$	OFF	OFF	ON	ON	ON	ON	OFF	OFF
$V_1 = E$	OFF	OFF	OFF	ON	ON	ON	ON	OFF
$V_0 = 0$	OFF	OFF	OFF	ON	ON	ON	ON	ON

The structure of single-phase k-level CMLI is shown in Fig. 7, and each H-bridge has a separate DC source. The inverter level can generate three voltages $+E$, 0, and $-E$ in each Cascaded H-Bridge (CHB) inverter. If S_1 and S_4 are on for $+E$ present in switches, if S_2 and S_3 are on $-E$ occurs in switches; if the output is 0V, all the switches are on. If the inverted voltage output of individual inverter levels is connected in series, then the output voltage is synthesized with the sum of all individual inverter levels. For the CHB inverter, the output voltage level 'k' is given ($k = 2s + 1$) where 's' is a number of separate DC sources.

The Fourier transform for the waveform shown in Fig. 8(a) is given as

$$\vartheta(wt) = \frac{4E}{\pi}\sum_{\rho}[cos(\rho\varphi_1) + cos(\rho\varphi_2) + \cdots + cos(\rho\varphi_s)]\frac{sin(\rho wt)}{\rho} \quad (1)$$

Equation (1) can be normalized with respect to E is given as

$$\aleph(n) = \frac{4}{\pi\rho}[cos(\rho\varphi_1) + cos(\rho\varphi_2) + \cdots + cos(\rho\varphi_s)] \quad (2)$$

Where $\rho = 1, 3, 5, 7, \ldots$:

$\varphi_1, \varphi_2, \cdots$ can be selected with harmonics reduction. CMLI can be connected to a star or delta connection with Static VAR, renewable energy sources, battery applications, etc. Fig. 8(b) shows 5L-CMLI voltage output with two DC sources and two H-bridges. The total output voltage is given as $V_{ao} = V_{a1} + V_{a2}$.

The most popular multi-level inverter topologies are NPC, FC, and CHB. In industrial applications, the author reviewed several MLI

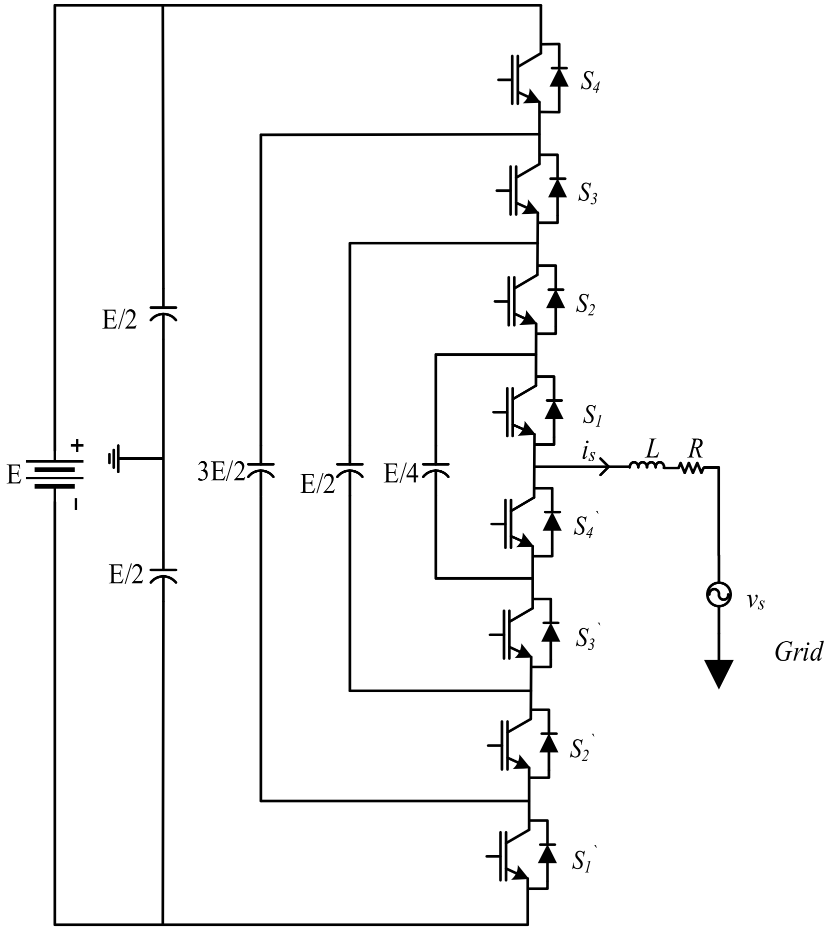

Fig. 6. Single phase 5-level FC inverter.

Table 3
Single phase 5-level FC inverter switching states.

Output Voltage (V)	Switching states							
	T_4	T_3	T_2	T_1	T_4`	T_3`	T_2`	T_1`
E	ON	ON	ON	ON	OFF	OFF	OFF	OFF
$E/2$	OFF	ON	ON	ON	ON	OFF	OFF	OFF
$-E/2$	ON	ON	OFF	OFF	OFF	OFF	ON	ON
-E	ON	OFF	OFF	ON	OFF	ON	ON	OFF
0	OFF	OFF	OFF	OFF	ON	ON	ON	ON

topologies and provided the specifications for commercial purposes. NPC has gained popularity in industrial applications due to its basic transformer structure. Higher levels of NPC are less popular due to uneven higher loss distribution. CHB is the perfect approach for high-voltage applications due to its modular structure. However, CHB requires isolated DC sources, which is expensive compared to NPC topology. FC contains a modular structure due to its switching frequencies; it is not popular in industrial applications. This work will pave the way for future improvements in CMLI.

2.2.1.1. Advantages of CMLI. The major advantages of CMLI's are shown below.

a) CHB structure provides high voltage switching with lower voltage ratings.
b) In CHB, several H-Bridge modules are connected in series, so output voltage levels are high.
c) The output voltage of the CMLI is twice that of the input DC sources, i.e., $(k = 2s + 1)$.
d) It produces the common mode voltage with reduced stress.

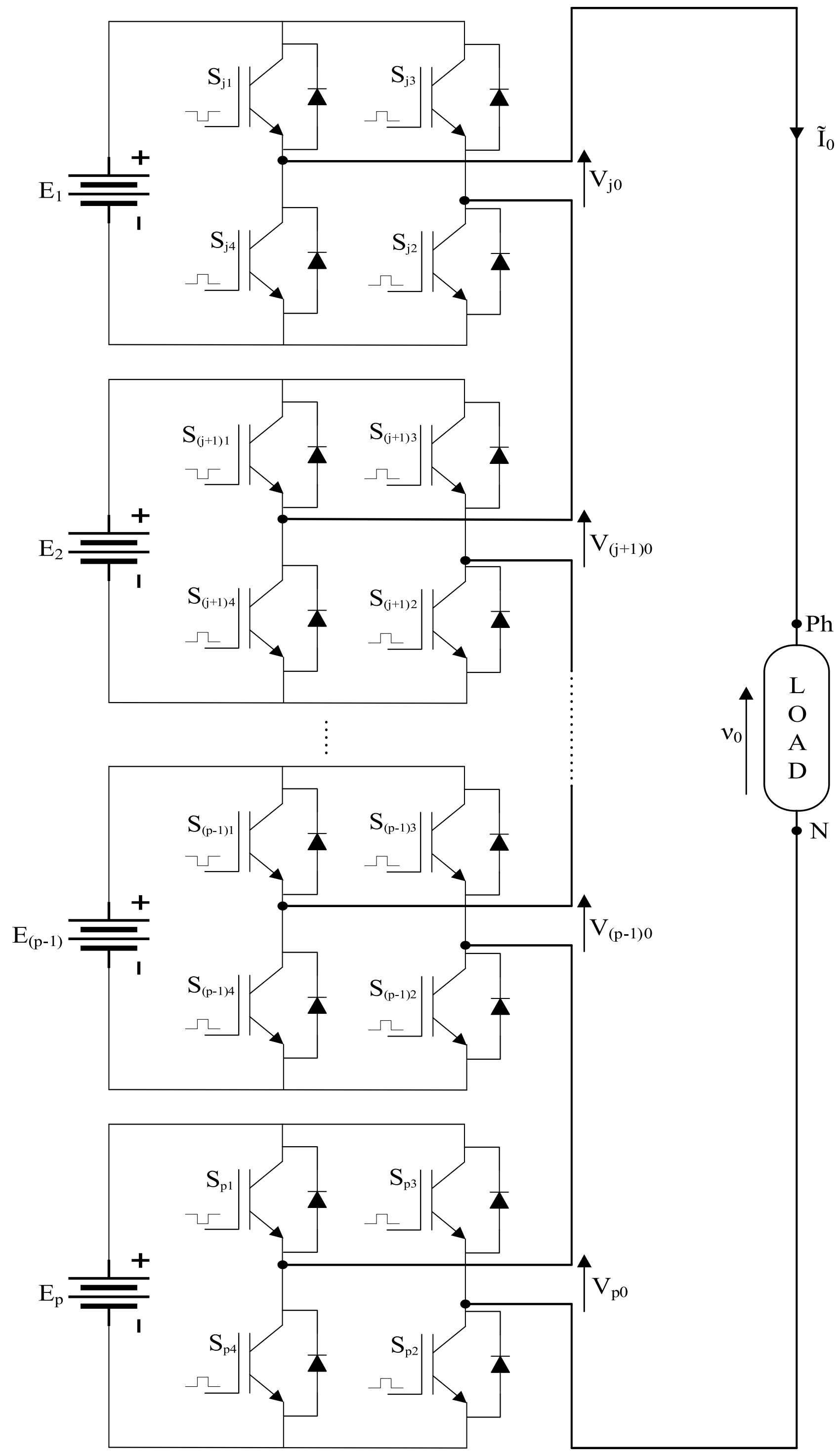

Fig. 7. Single phase structure of a CMLI.

e) CHB gains less input current with harmonic distortion.

2.2.2. Multi-level modulation of CMLI

The conventional sinusoidal PWM has two major types which can be defined as LS-PWM (Level Shifted) and PS-PWM (Phase Shifted). PS-PWM is commercially used in the CHB. PS-PWM triangular and sinusoidal waves are used. In triangular carriers'

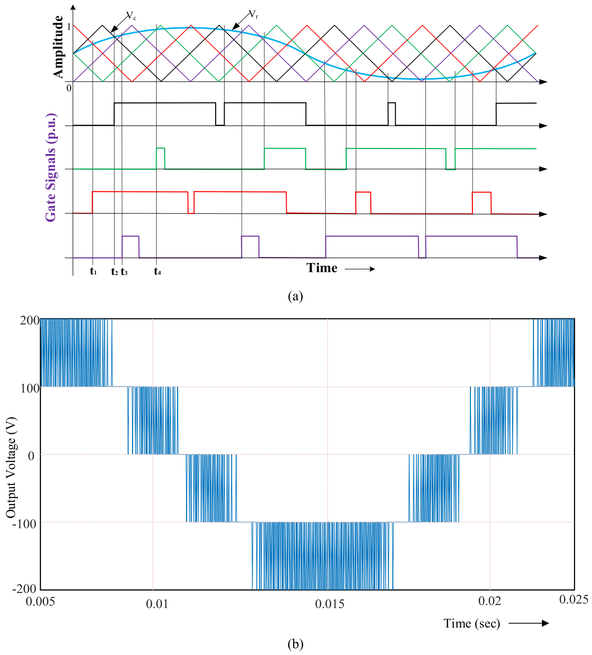

Fig. 8. (A) Gate pulse signals and (b) Ideal 5L arm voltage waveform.

magnitude is same and phase shift is 180°. Equation (3) shows the relation between the number of voltage levels and number of carriers.

$$\eta_c = \eta_{level} - 1 \tag{3}$$

$$\varphi_c = \frac{360^0}{\eta_{level} - 1} \tag{4}$$

$$m_f = \frac{f_c}{f_a} \tag{5}$$

$$m_a = \frac{\widehat{V_{ma}}}{\widehat{V_{cr}}} \tag{6}$$

φ_c is the phase difference between carriers, which is represented in Equation (4); the modulation index for both frequency (m_f) and amplitude (m_a) are calculated according to Equation (5) and Equation (6). The switching frequency (f_{sw}) of the PWM signal is equal to carrier frequency (f_c). The line-to-line voltage is twice the (η_c) with respect to switching frequency $\left(f_{eq} = \eta_{carrier} * f_c\right)$.

Harmonic components of CMLI are given as,

$$V_{an}(t) = \frac{E}{2} + \frac{E}{2}\left(cos(\mu_O t + \delta_o) + \frac{2E}{\pi}\sum_{\tau=1}^{\infty}\frac{1}{\tau}J_o\left(\tau\frac{\pi}{2}\mathrm{C}\right)*sin\left(\tau\frac{\pi}{2}\right)*cos(\tau(\mu_c t + \delta_c)) + \frac{2E}{\pi}\sum_{\tau=1}^{\infty}\right.$$
$$\left.\times\sum_{n=-\infty}^{\infty}\frac{1}{\tau}J_n\left(\tau\frac{\pi}{2}\mathrm{C}\right)*sin\left((\tau+n)\frac{\pi}{2}\right)*cos(\tau(\mu_c t + \delta_c) + n(\mu_c t + \delta_o)\right) \tag{7}$$

In Equation (7), sideband, baseband, carrier, and dc offset harmonics are presented. These harmonics can be canceled by shifting the carrier by $\frac{2\pi(i-1)}{N}$. The overall phase voltage is given as

$$\vartheta_{RP}(t) = \sum_{i=1}^{P}\vartheta_{Rp}^{i}(t) \tag{8}$$

Substituting Equation (7) – Equation (8) gives:

Table 4
High-performance MLI applications based on topology.

Application	Topology		
	NPCI/ANPCI	FCI	CMLI
Automotive Applications	[17]	[18–20]	[21–24]
HVDC	[25]	[26–28]	–
Wind power	[29–31]	[32]	–
Class-D Amplifiers	–	[42–44]	–
STATCOM	[45–47]	[26,48,49], 3 [6,50–53]	–
Locomotive (Train traction)	[54,54–58]	[54,55,58–63]	[64,65]
Photovoltaic	[66–68]	[59,66,67,69]	[70]
Regenerative Conveyors	[71,72]	–	–
Marine Propulsion	[67,68], [73,74]	[67,74]	[74]
Active filters	[75–79]	[80–82]	[83,84]
FACTS & Generation	[16]	[16,69,85,86]	[16]
UPQC, UPFC& DVR	[87–89]	[87,89,90]	[91]
Hydro-pumped storage	[92]	–	–

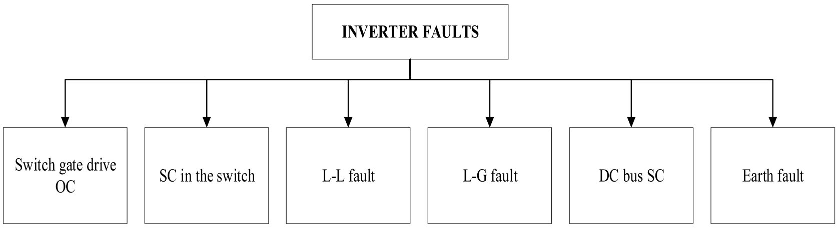

Fig. 9. Various inverter faults.

$$\vartheta_{RP}(t) = \frac{E.N}{2} + \frac{E.N}{2}\mathrm{C}cos(\mu_o t + \delta_o) + \frac{2E}{\pi}\sum_{i=1}^{N}\sum_{\tau=1}^{\infty}\frac{1}{\tau}J_o\left(\tau\frac{\pi}{2}\mathrm{C}\right)*sin\left(\tau\frac{\pi}{2}\right)*cos\left(\tau\left(\mu_c t + \frac{2\pi(i-1)}{N}\right)\right) + \frac{2E}{\pi}\sum_{i=1}^{N}\sum_{\tau=1}^{\infty}$$
$$\times \sum_{n=-\infty}^{\infty}\frac{1}{\tau}J_n\left(\tau\frac{\pi}{2}\mathrm{C}\right)*sin\left((\tau+n)\frac{\pi}{2}\right)*cos\left(\tau\left(\mu_c t\frac{2\pi(i-1)}{N}\right)n(\mu_o t + \delta_o)\right) \quad (9)$$

- Applications of MLI

MLI seeks attention for industries and academia due to its wide range of applications. MLI's are used in high power applications. MLI current commercial applications are grinding mills, pumps, fans, reactive power compensators, crushers, conveyor belts, solar, wind power conversations and so on. Research status of applications of MLI is tabulated in Table 4.

3. Fault diagnosis in CMLI

In 1994, Kastha and Bose classified fault diagnosis in CMLI as to be anticipated for the reliable operation of the system in the inverter, as shown in Fig. 9.

SC faults can be protected with circuit breakers, but faults associated with power semiconductor switches, i.e., IGBT, have to be anticipated. Different faults in the Inverter switches can be categorized in the following Table 5.

3.1. Diagnosis of faults & techniques

3.1.1. Introduction of various faults

Any unsatisfactory changes in the system are called a fault. Physical failures cannot be described as faults, but the term failure is a serious unconditional circumstance, breakdown, or deviation of the system. Different types of basic faults are shown in Fig. 10.

Table 5
Faults associated with the inverter switches.

S. No	OC Faults	SC Faults
1	One switch (upper or lower)	One switch (lower or upper)
2	Different phases (same side)	Two switches for different phases (same side of DC bus)
3	Different phases (different sides)	Two switches for different phases (different sides of the DC bus)

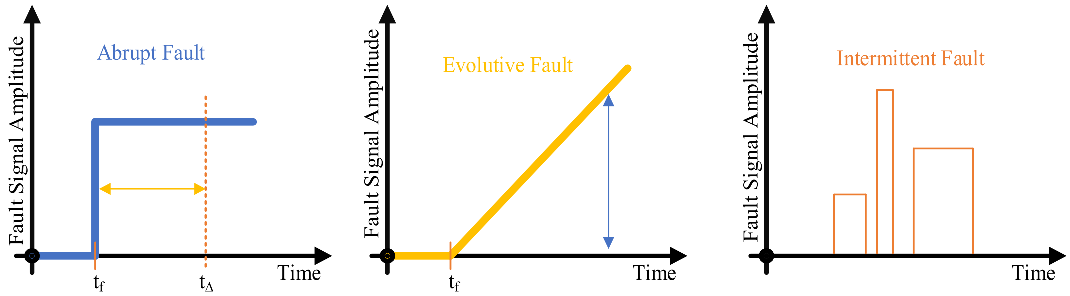

Fig. 10. Basic types of faults.

- Incipient Fault: It is a continuous fault that gradually develops. It can also be described as a soft fault or Evaluative fault.
- Abrupt Fault: These are substantial and immense faults that lead the system close to the acceptable limit.
- Intermittent Fault: These faults affect the system at discontinuous periods of time.

These faults are to be diagnosed as they affect the system's reliability, performance, and efficiency. Therefore, system monitoring is needed to assess the system's performance and to accurately diagnose faults at early stages.

Fault diagnosis system performs the following tasks.

- Fault Detection: Indication of occurrence of fault.
- Fault Isolation: Fault location determination.
- Fault Identification: Identification of the nature and size of the fault.

3.1.2. Classification of faults in dynamic system

The dynamic system faults can be divided into two parts open loops and close loops, which have further three important classifications can be described as sensor, actuators and plants. Closed loop dynamic system consists upon feedback controller. Fig. 11 shows the open loop dynamic system and Fig. 12 shows the closed loop dynamic system.

Fault diagnosis systems at each stage of open loop dynamic systems are required to evaluate system performance.

3.1.2.1. Sensor faults. Output interfaces that provide information about the system's internal behavior are called sensors. Sensor faults decrease system performance, such as data integrity of decision-making, decision-making systems, quality control systems, safety control systems, navigation, feedback control systems, state estimations, navigations, optimization systems, etc. Fault diagnosis in the sensors is required for accurate diagnosis and efficient control. The common faults in the sensors are.

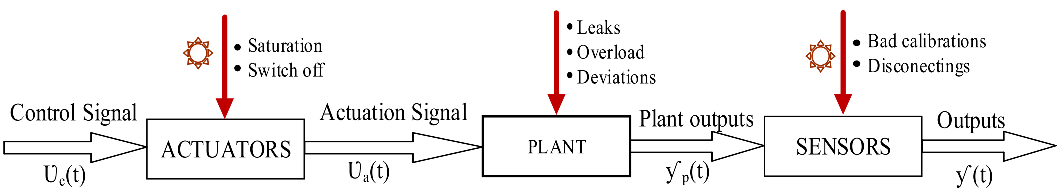

Fig. 11. Open loop dynamic system.

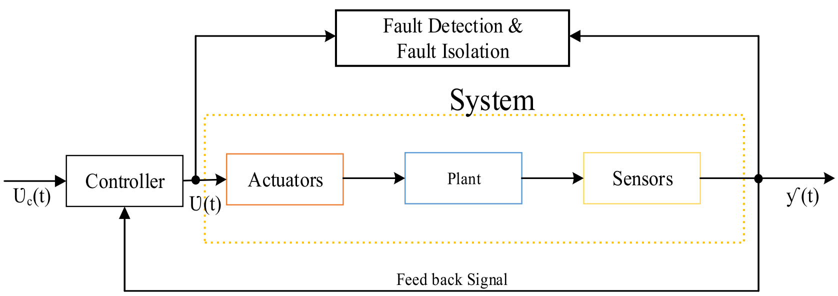

Fig. 12. Closed loop dynamic system.

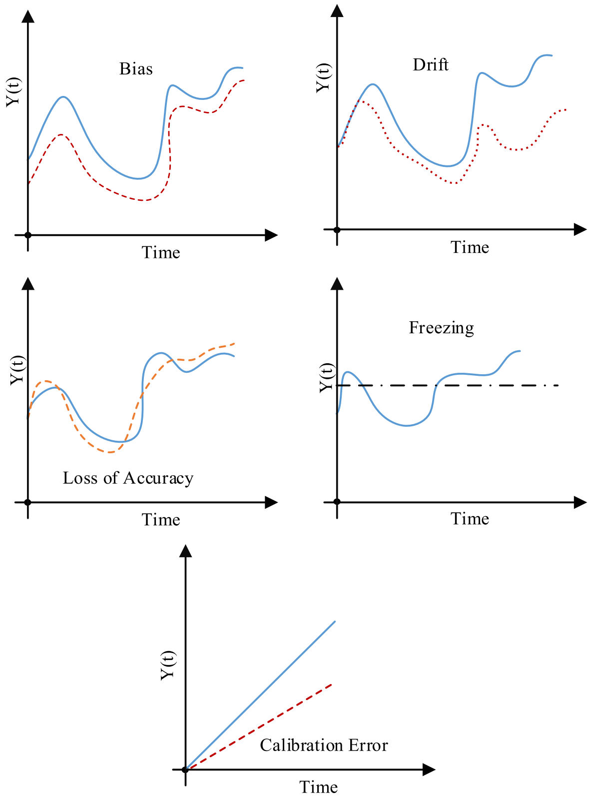

Fig. 13. Various sensor faults according to time.

- ➢ Bias
- ➢ Sensor Freezing
- ➢ Drift
- ➢ Calibration error
- ➢ Loss of accuracy or Performance degradation

The effect of various faults on the system measurements is shown in the following Fig. 13. The mathematical representation of the Sensor faults is shown in Equation (10) as follows:

$$\mathrm{y_i(t)} = = \begin{cases} \varnothing_i(t) & \varnothing_i \neq 0 & \forall \alpha \geq \alpha_0 & \text{No failure} \\ \varnothing_i(t) + a_i & a_i(\alpha) = 0, a_i(\alpha_{Fi}) \neq 0 & \forall \alpha_{Fi} < \alpha & \text{Bias} \\ \varnothing_i(t) + a_i(\alpha) & |a_i(\alpha)| = c_i(t\alpha), 0 < c_i \ll 1 & \forall \alpha \geq \alpha_{Fi} & \text{Drift} \\ \varnothing_i(t) + a_i(\alpha) & |a_i(\alpha)| \leq \overline{a}_i, \dot{a}_i(\alpha) \in L^\infty & \forall \alpha \geq \alpha_{Fi} & \text{accuracy fault} \\ \varnothing_i(\alpha_{Fi}) & \varnothing_i \neq 0 & \forall \alpha \geq \alpha_{Fi} & \text{Sensor fault} \\ k_i(\alpha)\varnothing_i & 0 < \overline{k} \leq k_i(\alpha) \leq 1 & \forall \alpha \geq \alpha_{Fi} & \text{Calibration Error} \end{cases} \tag{10}$$

Where, α_{Fi}: Denotes the fault at ith sensor unit.

a_i: Accuracy coefficient $a_i \in (-a_i, a_i)$.

$k_i \in (k_i, 1)$, $k_i > 0$ represents minimum sensor effectiveness.

The generalized mathematical model is represented by:

$$Y = K_m X + B \tag{11}$$

Where.

K_m: Positive definite diagonal matrix varies slowly between $(k_i, 1)$.

B: Matrix B varies slowly between $(-a_i, a_i)$.

3.1.2.2. Component faults. Component faults occur when the nominal conditional changes occur in the systems. Some examples for this fault are.

- ➢ Power source failure in the satellite.

Table 6
Different faults in the actuator.

S. No	Actuator Type	Fault
1.	Control valve actuators	✓struck open ✓struck close ✓Abnormal Leakage
2.	Servo motor actuators	•Lock-in Phase (LIP) or Freezing •Loss of Effectiveness (LOE) •Float •Hard Over Failure (HOF)

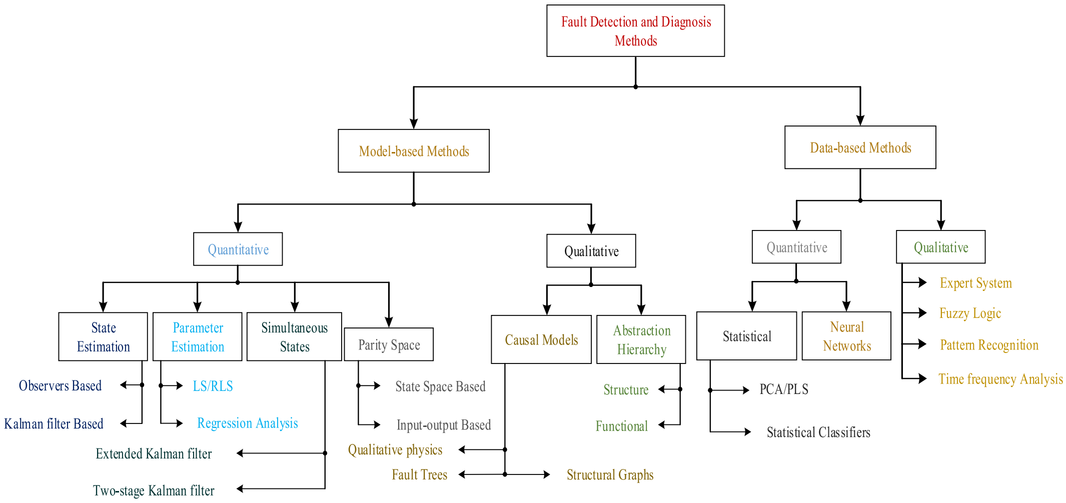

Fig. 14. Different fault detection and diagnosis methods.

➢ Leakage in the tank of the propulsion system or chemical system.
➢ Body damage faults.
➢ Friction faults due to lack of lubrication.
➢ Breakage and crack in the gear system, etc.

The mathematical modeling of component faults is very difficult, and experimentation is needed to model the component fault state equation used generally.

3.1.2.3. Actuator faults. In electromechanical or electrochemical systems, actuator transpires the control signals from microprocessor or microcontroller to attain appropriate signals i.e. force, torque etc. to drive the system. Hence abnormalities in the actuators lead to the absolute loss and high energy consumption of the system. Actuator faults depend on the type of actuator system. Examples of the actuator faults are tabulated in Table 6.

LIP fault freezes the actuator and does not respond to commands. Float occurs in the actuator at zero moment. LIE fault reduces the actuator gain. The mathematical representation of actuator faults is represented by following Equation (12)

$$y_i(t) = \begin{cases} u_c^i(\theta) & Absece\ of\ Faults \\ \sigma_i(\theta)u_c^i(\theta) & 0 < \in_i \le \sigma(\theta) < 1, \forall\theta \ge \theta_{Fi}; (LOE) \\ 0 & \forall\theta \le \theta_{Fi}; (Float) \\ u_c^i(\theta_{Fi}) & \forall\theta \le \theta_{Fi}; (LIP) \\ u_{i\ min} \bigvee u_{i\ max} & \forall\theta \le \theta_{Fi}; (HOF) \end{cases} \tag{12}$$

Where $u_a^i(t)$: Actuation signal.
$u_c^i(t)$: Control command signal.
θ_{Fi}: Denotes the time of fault occurrence at ith actuator.
$\sigma_i \in (\in_i, 1), \in_i > 0$ represents minimum actuator effectiveness.
$u_{i\ min}$ and $u_{i\ max}$ are the actuator's limits.
The generalized equation of the actuator is shown in the following Equation (13)

Table 7
Existing literature in FDI methods for PE system.

Parameters	Switch Fault	Multiple Switch Fault	Open Phase	Sensor Fault	Passive Element Fault
Hardware-based (Analog Circuits)	[93–99]	[96]	[94]	–	–
Model-based	[100–110]	[111,112]	[100]	[113]	[114,115,117,118]
Signal Processing (Time Domain)	[108–110]	[116,122–126]	[127]	–	–
Signal Processing (Freq. domain)	[128–133]	[108]	[130]	[131]	–
Statistical	[130,134]	–	[101]	–	–
Machine Learning	[128,129,133,134,137,138–141]	[108,126,142]	[143]	–	–
Hidden Markov Model	[135]	[144]	–	–	–

$$u_a^i(t) = \delta_i \sigma_i u_c^i(\theta) + (1 - \delta_i)\overline{u_i} \tag{13}$$

Where,

$\delta_i = 1, \sigma_i = 1$ at zero faults.

$\delta_i = 1, 0 < \sigma_i < 1$ in the presence of LOE.

$\delta_i = 0$ for other faults, such as u_i is in a position the actuator is locked.

3.2. Different types of fault diagnosis techniques

3.2.1. Classifications of fault diagnosis methods

The fault diagnosis methods are classified into two types, which can be delineated as Model-based methods and Data-based methods. Further, these methods are subdivided into qualitative and quantitative methods. Model-based methods consist of state estimation, parameter estimation, simultaneous estimation, parity space, etc. Data-based methods consist of statistical, neural networks, expert systems, fuzzy logic, pattern reorganization, qualitative trend analysis, etc. The detailed classification of fault diagnosis methods is shown in Fig. 14.

3.2.2. Research status

Researchers [93–99] depicted hardware-based switch faults, multiple switch faults, and open phase faults. Model-based analysis of switch faults, multiple switch faults, open phase faults, sensor faults, and passive element faults are presented in Refs. [100–117]. Signal processing with time domain analysis for switch faults, multiple switch faults, and open phase faults presented by Refs. [118–127]. Signal processing with frequency domain analysis for switch faults, multiple switch faults, open phase faults, and sensor faults is studied in Refs. [108,128–133]. Statistical analysis for switch faults and open phase faults is presented in Refs. [101,130–134].

Machine learning based analysis for switch faults, multiple switch faults and open phase faults presented by Refs. [101,108,126,130,133]. Hidden Markov Model is presented in Refs. [135,136]. The detailed research status is in Table 7.

4. Power inverter IGBT fault diagnosis

IGBT's are widely used as a power inverter in several high-power applications. It is anticipated from Ref. [145] that the occurrence of a fault in power switching devices will be 38 %. Almost all power inverters and IGBTs are used as switching devices due to their characteristics. IGBT can handle the short circuit current of more than 10μs. IGBT failures happen due to thermal and electrical stresses. That's why an IGBT fault diagnosis system is needed. IGBT fault diagnosis is classified as given below.

- OC Faults
- SC Faults
- Intermittent Gate-Misfiring Faults

4.1. OC faults

The OC fault is considered a gate-driven OC fault because of bond wire lift-off due to thermal cycling. OC fault in IGBT creates a DC offset current in the healthy and fault phases. This DC current leads to the uneven distribution of stress. OC fault doesn't shut down the system, but it degrades system performance. That's why a fault diagnosis system is essentially required. Different fault diagnosis methods are summarized in Table 8 below.

4.2. SC faults

In the IGBT SC, a fault occurs due to the following reasons.

- Incorrect gate voltage or dv/dt disturbance.
- Over voltage/avalanche stress or temperature overshoot.

Table 8
OC fault diagnosis methods.

FD Methods	Comments	References
Park's Vector Method	-Detection Time: 20.0 ms. -Detection parameters: 3-Φ Currents. - Implementation Procedure: Medium risk. - Tuning Effort Range: Long range. - Threshold dependence is: High level. - Merits/Demerits: Ambiguous effectiveness, Poor resistivity.	[146]
Modified Normalized DC Current Method	✓ Detection Time: 18.4 ms. ✓ Detection parameters: 3 phase Currents. ✓ Implementation Procedure: Low risk. ✓ Tuning Effort Range: Short range. ✓ Threshold dependence is: Independent to each other. ✓ Merits/Demerits: Good effectiveness, Good resistivity.	[147]
Normalized DC Current Method	- Detection Time: 13.8 ms. - Detection parameters: Three-phase currents. - Implementation Procedure: Low risk. - Tuning Effort Range: Short range. - Threshold dependence is: Independent to each other. - Merits/Demerits: Poor effectiveness, Poor resistivity.	[148]
AC Current Space Vector Instantaneous Frequency Method	✓ Detection Time: 20.0 ms. ✓ Detection parameters: 3-Φ Currents. ✓ Implementation Procedure: Low risk. ✓ Tuning Effort Range: Short range. ✓ Threshold dependence is: Low level. ✓ Merits/Demerits: Medium resistivity.	[149,150]
Centroid-Based Fault Detection	- Detection parameters: 3-phase Currents - Implementation Procedure: Highly risk. - Tuning Effort Range: Medium range. - Threshold dependence is: Dependent to each other. - Merits/Demerits: Good effectiveness and Good resistivity.	[151]
Diagnosis by Sensing Voltage Across Lower Switch	✓ Detection Time: 2.7 ms. ✓ Detection parameters: Low switching voltages. ✓ Implementation Procedure: Medium risk. ✓ Tuning Effort Range: Long range. ✓ Threshold dependence is: Independent to each other. ✓ Merits/Demerits: Good effectiveness and Good resistivity.	[152]
Current Pattern Recognition Method in the Time Domain	- Detection Time: 10.0 ms. - Detection parameters: Three-phase currents. - Implementation Procedure: Low risk. - Tuning Effort Range: Medium range. - Threshold dependence is: High level. - Merits/Demerits: Medium resistivity.	[153]
Spectrum Analysis Method	✓ Detection Time: 2.0 ms. ✓ Detection parameters: 3-phase Currents. ✓ Implementation Procedure: Highly risk. ✓ Tuning Effort Range: Both short and long range. ✓ Threshold dependence is: High level. ✓ Merits/Demerits: Good effectiveness and Medium resistivity.	[154]
Current Deviation Method	- Detection Time: 6.87 ms. - Detection parameters: Three-phase currents. - Implementation Procedure: Highly risk. - Tuning Effort Range: Short range. - Threshold dependence is: Independent to each other. - Merits/Demerits: Good effectiveness and Medium resistivity.	[155]
Wavelet-Fuzzy Algorithm	✓ Detection time: 5.0 ms. ✓ Detection parameters: 3-Φ Currents. ✓ Implementation Procedure: Highly risk. ✓ Tuning Effort Range: Medium range. ✓ Threshold dependence is: Low level. ✓ Merits/Demerits: Good effectiveness and Good resistivity.	[156]
Wavelet-Neural Network Method	- Detection parameters: Three-phase currents. - Implementation Procedure: Highly risk. - Tuning Effort Range: Short range. - Merits/Demerits: Good effectiveness NN is trained effectively.	[157]
Subtractive Clustering-Based Mean Current Vector Method	✓ Detection time: 0.25 ms. ✓ Detection parameters: 3-Φ Currents. ✓ Implementation Procedure: Low risk. ✓ Tuning Effort Range: Medium range. ✓ Merits/Demerits: Good effectiveness.	[158]

(*continued on next page*)

Table 8 (*continued*)

FD Methods	Comments	References
Wavelet-ANFI System	- Detection parameters: DC link currents. - Implementation Procedure: Highly risk. - Tuning Effort Range: Short range. - Threshold dependence is: Independent to each other. - Merits/Demerits: Good effectiveness.	[159]
Clustering-ANFI System	✓ Detection parameters: 3-Φ Currents. ✓ Implementation Procedure: Highly risk. ✓ Tuning Effort Range: Low range. ✓ Merits/Demerits: Good resistivity.	[160]
Model-Based ANN Diagnostic Method	- Detection parameters: Three-phase currents, voltages, and torque. - Implementation Procedure: Highly risk. - Tuning Effort Range: Medium range. - Threshold dependence is: Independent to each other. - Merits/Demerits: Medium resistivity.	[161]
Using the Bond Graph Model	✓ Detection parameters: Switch Voltages. ✓ Implementation Procedure: Highly risk. ✓ Threshold dependence is: High level. ✓ Merits/Demerits: Good effectiveness.	[162]

Table 9
SC fault diagnosis methods.

FD Methods	Comments	References
Current Mirror Method	❖ It requires the device's current parameter. ❖ It has an abrupt turn-off. ❖ Implementation effort is low, and reliability is medium.	[163]
De-Saturation Detection	➢ It requires a collector voltage parameter. ➢ It has an abrupt turn-off. ➢ Implementation effort is low, and reliability is medium.	[164]
Vector Composition of Inverter Output Voltage	❖ It requires an inverter output voltage parameter. ❖ Implementation effort is Medium, and reliability is Low.	[165]
Gate Voltage Sensing	➢ It requires a gate voltage parameter. ➢ It has an abrupt turn-off. ➢ Implementation effort is low, and reliability is low.	[166]
di/dt feedback Control	❖ It requires the device's current parameter. ❖ It has a soft turn-off. ❖ Implementation effort is high, and reliability is medium.	[167]
Average Current Park's Vector Approach	➢ It requires a phase current parameter. ➢ Implementation effort is medium, and reliability is high.	[168]

SC faults are complex in nature and take time for fault initiation, and their failures are very few. That's why a fault diagnosis system is extremely needed to manage the system performance and eviction. Different fault diagnosis methods are summarized in the following Table 9.

4.3. Intermittent Gate-Misfiring Faults

An intermittent gate-misfiring fault leads the system toward a breakdown. It may be caused by factors such as electromagnetic compatibility degradation, element deterioration in the control circuit, and driver circuit opening. However, the power inverter can operate up to an accountable period with decreased output. Intermittent gate-misfiring Faults also lead towards the SC fault and are intermittent in nature. Detection by output current trajectory [169] and pattern recognition approach [170,163] are the diagnosis methods for gate-misfiring fault in the time domain, as frequency domain diagnosis methods are not suitable.

4.4. Reliability of fault detection system

The reliability of the fault detection system has to be anticipated in system error analysis. A reliability-based fault management system has to be designed for diagnosis.

A fault detection approach can protect the system from greater damage by isolating the faulty locations. The fault detection approach is based on two types.

1. Online Approaches
2. Offline Approaches

Table 10
Online fault detection approaches.

Online Approaches	Remarks	Reference
Centralized	Base station plays active role in the detection of fault.	[167]
Neighborhood-coordination-based	➢ Localized fault-tolerant event boundary detection. ➢ 2-ΦNeighbor co-ordination scheme. ➢ Distributed fault detection of wireless sensor networks.	[168]
Cluster-based	❖ Heart-beat based. ❖ Polling-based.	[171]

Table 11
Comparison of fault detection methods.

Method	Remarks	Reference
Neural Networks	Overall Efficiency: without noise is 95.00 %	[172]
Temporal attribute QSSVM	Overall Efficiency: without noise is 98.10 %	[173]
Wavelet-based fuzzy logic theory	Overall Efficiency: without noise is 100.00 %	[174]
SVM-based principal components analysis	Overall Efficiency: a Without noise is 99.74 % b With noise is 99.79 % at 30 dB c With noise is 99.77 % at 20 dB	[175]
Hybrid ST method	Overall Efficiency: a Without noise is 100 % b With noise is 100 % at 40 dB, 30 dB, 20 dB for both balanced and unbalanced loads. c Multiphase systems efficiency is 99.90 % at 40 dB, 99.70 % at 30 dB, 99.60 % at 20 dB	[176]
Artificial Neural Network	Focuses on fault detection in asymmetric multilevel inverters, demonstrating the utility of neural networks with systems efficiency of 98.89 % (without Noise)	[36]
FFT-RPCA-SVM Diagnosis Method	Introduces a novel diagnosis method based on frequency domain analysis, enhancing fault detection in multilevel inverters with efficiency 99.74 % (without noise)	[37]
Sparse Representation and Deep Learning	Reiterates the combination of sparse techniques and deep learning for effective fault diagnosis with efficiency of 99.77 % (at 20 dB)	[177]
Improved Support Vector Machine with Gray Wolf Algorithm	Enhances fault diagnosis in H-bridge cascaded five-level inverters, demonstrating optimization capabilities with efficiency of 100 % (without noise)	[38]
Artificial Neural Networks for Fault Recognition	Novel approach using ANNs for fault recognition in multilevel inverters, enhancing diagnostic methods with efficiency of 99.42 % (without noise)	[41]

Table 12
Comparison of fault classification methods.

Method	Remarks	Reference
Wavelet-based fuzzy logic theory	Overall Efficiency: without noise is 89.50 %	[178]
Wavelet multi resolution method	Overall Efficiency: without noise is 94.73 %	[178]
Wavelet-based ANFIS	Overall Efficiency: without noise is 99.84 %	[179]
Wavelet-based ANN	Overall Efficiency: without noise is 98.40 %	[180]
Time transformation-based ART NN	Overall Efficiency: without noise is 99.18 %	[180]
Attribute QSSVM method	Overall Efficiency: without noise is 99.05 %	[181]
SVM-based principal components analysis	Overall Efficiency: without noise is 99.93 %	[181]
Hybrid ST method	Overall Efficiency: a Without noise is 99.95 % b With noise is 99.75 % at 40 dB, 99.85 % at 30 dB, and 99.80 % at 20 dB for both balanced and unbalanced loads c Multiphase systems efficiency is 99.33 % at 40 dB, 99.14 % at 30 dB, 99.02 % at 20 dB	[178, 180]
Multiscale Kernel Convolutional Neural Network	Fault diagnosis in cascaded multilevel inverter with 99.67 %.	[33,35]
Sparse Representation & Deep CNN	Intelligent diagnosis with high accuracy in cascaded H-bridge multilevel inverter with 99.72 %	[34,182]
Gray Wolf Algorithm with SVM	Fault diagnosis of H-bridge cascaded five-level inverter with 98.85 %	[38]
FFT-RPCA-SVM	Fault diagnosis method for cascaded multilevel inverter with 99.11 %	[37]
Rolling Average-Decision Tree	Fault detection method for neutral point clamped inverters with 98.85 %	[40]
Artificial Neural Networks (ANN)	Fault recognition in multilevel inverters through ANN with 99.30 %	[41]
Machine Learning Algorithms for Open Switch Fault	Fault diagnosis of cascade H-bridge multi-level inverter in distributed power generators with 98.87 %	[39]

Table 13
Comparative analysis of faults and diagnosis techniques in cascaded multi-level inverters.

Citation	Inverter Type	Fault Type Analyzed	Diagnosis Method	Algorithm Used	Accuracy (%)	Fault Detection Speed	Noise Sensitivity	Scalability	Computational Complexity	Real-Time Capability
Yang Z. et al., 2017 [158]	Induction Motor	Slip Compensation	Current Vector Decoupling	Vector Decoupling Control	Not Specified	Fast	Moderate	High	Moderate	Yes
Schlechtingen M. et al., 2013 [159]	Wind Turbine	Power Curve Monitoring	Data-Mining Approach	Data Mining	93.0 %	Moderate	High	High	High	No
Feng Z.P. et al., 2015 [160]	Planetary Gearbox	Fault Diagnosis	Generalized Synchrosqueezing Transform	Signal Processing	95.0 %	Slow	High	Low	High	No
Feng Z. et al., 2004 [161]	General Mechanical Systems	Fault Diagnosis	Cluster Analysis + Rough Set + Fuzzy Neural Network	Fuzzy Neural Network	92.8 %	Moderate	High	Moderate	Moderate	No
Forrester J.W., 1990 [162]	Industrial Processes	System Modeling	Bond Graphs	Bond Graph Modeling	Not Specified	Slow	High	Low	High	No
Sicard E. et al., 1992 [169]	General Systems	Pattern Recognition	Real-Time Pattern Recognition	Custom Algorithms	Not Specified	Fast	Low	High	Low	Yes
Sasidharan A. et al., 2018 [170]	Banking Networks	Pattern Recognition	Pattern Recognition Algorithms	Machine Learning	Not Specified	Fast	Low	High	Moderate	Yes
Jose Luis RT. et al., 2018 [163]	Power Systems	Vulnerability Prediction	Pattern Recognition	Machine Learning	95.5 %	Moderate	High	High	High	No
Locher R.E., 1991 [164]	IGBTs	Overcurrent Protection	Short Circuit Proof	IGBT Modeling	Not Specified	Fast	Low	High	Low	Yes
Jha M.S. et al., 2014 [165]	Industrial Systems	Fault Identification	Bond Graph Model	Fault Detection	Not Specified	Moderate	High	Moderate	High	No
Perpina X. et al., 2008 [166]	Railway Applications	IGBT Module Failure	Failure Analysis	Failure Mode Analysis	Not Specified	Moderate	Low	Moderate	High	No
Hu Y. et al., 2014 [167]	Dual Three-Phase Motors	Current Unbalance & Harmonics	Current Control	Harmonic Compensation	96.7 %	Moderate	Moderate	High	Moderate	No
Cheong M. et al., 2019 [168]	Integrated Circuits	Fault Diagnosis	3D Rotation Based Architecture	Redundancy Architecture	Not Specified	Moderate	Low	Moderate	High	No
Abbasi A.R. et al., 2018 [171]	Power Transformers	Winding Fault Diagnosis	Cross-Correlation + Clustering	Clustering Analysis	93.5 %	Moderate	Moderate	High	High	No
Sun W.J. et al., 2016 [172]	Induction Motors	Fault Classification	Sparse Autoencoder	Deep Neural Network	97.3 %	Moderate	High	High	Moderate	Yes
Thakur V.S. et al., 2019 [173]	Image Compression	Fault Diagnosis	Nonnegative Integer Bit Allocation	Fuzzy Domain Estimation	Not Specified	Slow	Moderate	Moderate	High	No
Huang W. et al., 2018 [174]	General Systems	Fault Diagnosis	Hybrid Fuzzy Wavelet Neural Networks	Polynomial Neural Networks	96.0 %	Moderate	High	High	High	No
Abreu A.L.E. et al., 2018 [175]	Reservoirs	Evaporation Loss Prediction	Machine Learning	Regression Models	Not Specified	Slow	Moderate	High	High	No
Mathkour H. et al., 1995 [176]	Databases	Monitoring	Machine Learning	Neural Networks	Not Specified	Moderate	Low	Moderate	High	No
Jin-Shun F. et al., 2008 [178]	Wavelet Analysis	Pattern Recognition	Multiple Vector-Valued Wavelet Packets	Wavelet Packets	Not Specified	Slow	High	Moderate	High	No

(*continued on next page*)

Table 13 (*continued*)

Citation	Inverter Type	Fault Type Analyzed	Diagnosis Method	Algorithm Used	Accuracy (%)	Fault Detection Speed	Noise Sensitivity	Scalability	Computational Complexity	Real-Time Capability
Toda H. et al., 2009 [179]	Signal Processing	Pattern Recognition	Translation-Invariant Wavelet Packet Transforms	Wavelet Transforms	Not Specified	Slow	High	Moderate	High	No
Ahmed R. et al., 2018 [180]	Gear Monitoring	Fault Diagnosis	Wavelet-Based Denoising	Neural Networks	Not Specified	Moderate	High	Moderate	High	No
Cruz S.M.A. et al., 2001 [181]	Synchronous & Asynchronous Motors	Winding Fault Diagnosis	Extended Park's Vector Approach	Vector Analysis	94.2 %	Fast	Moderate	High	Low	Yes
Sivapriya, A. et al., 2023 [33]	Cascaded Multilevel	Various Faults	Enhanced Deep Learning	CNN	98.5 %	Fast	High	Excellent	Moderate	Yes
Sivapriya, A. et al., 2023 [34]	Cascaded Multilevel	Switch Faults	Multiscale Kernel CNN	CNN	97.8 %	Moderate	Moderate	High	Moderate	Yes
Du, B. et al., 2023 [35]	H-Bridge Multilevel	Open-circuit & Short-circuit	Sparse Representation + CNN	Sparse Representation, CNN	96.5 %	Moderate	High	High	High	Limited
Yuan, Q. et al., 2023 [38]	H-Bridge Cascaded Five-level	Switch Faults	SVM + Gray Wolf Algorithm	SVM, Gray Wolf	95.2 %	Moderate	Moderate	Moderate	High	Limited
Raj, N. et al., 2018 [36]	Asymmetric Multilevel	Switch Faults	Artificial Neural Network	ANN	94.7 %	Fast	Moderate	Moderate	Moderate	Yes
Wang, T.Z. et al., 2016 [37]	Cascaded Multilevel	Switch Faults	FFT-RPCA-SVM	FFT, RPCA, SVM	93.4 %	Slow	High	Low	High	Limited
Ali, M. et al., 2021 [39]	H-Bridge Multilevel	Open-switch Faults	Machine Learning Algorithms	Decision Tree, KNN	92.0 %	Moderate	Low	Low	Low	Yes

4.4.1. Online Approaches

Online fault detection approaches are used to find the fault during real-time detection. Sanity check and network faults are commonly detected in online faults. Sanity check detects the parameters like temperature levels, energy level etc. Network fault is related to network issues like status of sensor nodes, links, frequency route changes, loss rate, internet faults etc. Online fault detection approaches are tabulated in the following Table 10.

4.4.2. Offline Approaches

Offline fault detection is a complex approach because it has to backtrack and reconstruct a complete system procedure. Offline approach: about detection and classification of fault, i.e., useful features are extracted from feature extraction; the fault is classified. The comparison for the fault detection method is tabulated in Table 11. The comparison for the fault detection method is tabulated in Table 12.

5. Conclusion

This paper presents a thorough analysis of the 5-Level Cascaded Multilevel Inverter (5L-CMLI) under various fault conditions, emphasizing the significance of fault diagnosis techniques (see Table 13). The first section introduces inverter technology and outlines the importance of this study in improving the reliability of multilevel inverters used in critical applications such as renewable energy and electric vehicles. The second section describes different types of multilevel inverters, their advantages and disadvantages, and their applications across industries. A comprehensive literature review identifies existing fault diagnosis methods and highlights gaps in current research. The third section summarizes various fault diagnosis techniques, distinguishing between open-loop and closed-loop dynamic systems. Advanced methods, including wavelet-based approaches and artificial intelligence (AI), are discussed for their effectiveness in accurately classifying faults. In the fourth section, common faults in Insulated Gate Bipolar Transistor (IGBT)-based converters are examined, focusing on contemporary R&D efforts aimed at enhancing fault detection. Finally, the paper compares the overall efficiency and reliability of different fault diagnosis methods, demonstrating that AI-based techniques, particularly those employing neural networks, significantly improve fault detection accuracy and operational efficiency in CMLIs. This study underscores the potential of integrating advanced technologies to enhance fault diagnosis systems in multilevel inverters, ultimately contributing to greater reliability in industrial applications.

CRediT authorship contribution statement

Ranjith Kumar Gatla: Writing – original draft, Methodology, Conceptualization. **Devineni Gireesh Kumar:** Investigation, Formal analysis, Data curation. **Palthur Shashavali:** Validation, Software, Resources. **Rao Dsnm:** Visualization, Validation, Conceptualization. **Hossam Kotb:** Resources, Project administration, Conceptualization. **Abdulaziz Alkuhayli:** Validation, Project administration, Formal analysis. **Yazeed Yasin Ghadi:** Validation, Project administration, Formal analysis. **Wulfran Fendzi Mbasso:** Writing – review & editing, Supervision, Project administration.

Data availability statement

The data are available from the corresponding author upon request.

Declaration of competing interest

The authors declare that they have no known competing financial interests or personal relationships that could have appeared to influence the work reported in this paper.

Acknowledgment

This work was supported by the Researchers Supporting Project number (RSP2024R258), King Saud University, Riyadh, Saudi Arabia.

References

[1] S. Payami, R.K. Behera, A. Iqbal, R. Al-Ammari, Common-mode voltage and vibration mitigation of a five-phase three-level NPC inverter-fed induction motor drive system, IEEE Journal of Emerging and Selected Topics in Power Electronics 3 (2) (2015) 349–361.
[2] H. Soliman, M. Shafiq, Robust. Stabilisation of power systems with random Abrupt changes, IET Gener. Transm. Distrib. 9 (15) (2015) 2159–2166.
[3] D.R. Espinoza-Trejo, D.U. Campos-Delgado, F.J. Martinez-López, Variable speed evaluation of a model-based fault diagnosis scheme for induction motor drives [C], in: IEEE International Symposium on Industrial Electronics, IEEE, 2010, pp. 2632–2637.
[4] Hamouda M. AbariI, B.H. SlamaJ, Open-switch Fault Detection in three-phase symmetrical cascaded multi-level inverter using conducted disturbances, International Multi-Conference on Systems, Signals & Devices.IEEE (2018) 77–82.
[5] Z. Zhang, F. Wang, L.M. Tolbert, et al., Evaluation of switching performance of SiC devices in PWM inverter-fed induction motor drives, IEEE Trans. Power Electron. 30 (10) (2015) 5701–5711.
[6] D.U. Campos-Delgado, J.A. Pecina-Sanchez, D.R. Espinoza-Trejo, R. Arce-SantanaE, Diagnosis of open-switch faults in variable speed drives by stator current analysis and pattern recognition, IET Electr. Power Appl. 7 (6) (2013) 509–522.

[7] M. Alavi, D. Wang, M. Luo, Short-circuit fault diagnosis for three-phase inverters based on voltage-space patterns, IEEE Trans. Ind. Electron. 61 (10) (2014) 5558–5569.
[8] R.A. Keswani, H.M. Suryawanshi, M.S. Ballal, Multi-resolution analysis for converter switch faults identification, IET Power Electron. 8 (5) (2015) 783–792.
[9] S. Ouni, M.R. Zolghadri, M. Khodabandeh, et al., Improvement of post-fault performance of a cascaded H-bridge multi-level inverter, IEEE Trans. Ind. Electron. 64 (4) (2017) 2779–2788.
[10] M. Aleenejad, AhmadiR, Fault-tolerant multi-level cascaded H-bridge inverter using impedance-sourced network, IET Power Electron. 9 (11) (2016) 2186–2195.
[11] M. Sahoo, S. Keerthipati, Fault tolerant three-level boost inverter with reduced source and LC count, IET Power Electron. 11 (2) (2018) 399–405.
[12] L. Liu, H. Li, S. Hwang, J. Kim, An energy-efficient motor drive with autonomous power regenerative control system based on cascaded multi-level inverters and segmented energy storage, IEEE Trans. Ind. Appl. 49 (1) (2013) 178–188.
[13] S. Sau, B.G. Fernandes, Modular multi-level converter based variable speed drive with reduced capacitor ripple voltage, IEEE Trans. Ind. Electron. 66 (5) (2019) 3412–3421.
[14] A.S. Gadalla, X. Yan, S.Y. Altahir, H. Hasabelrasul, Evaluating the capacity of power and energy balance for cascaded H-bridge multi-level inverter using different PWM techniques, J. Eng. 6 (13) (2017) 1713–1718.
[15] S. Munawar, M.S. Iqbal, M. Adnan, M. Ali Akbar, A. Bermak, Multilevel Inverters Design, Topologies, and Applications: Research Issues, Current, and Future Directions IEEE Access 12 (2024) 149320–149350, https://doi.org/10.1109/ACCESS.2024.3472752.
[16] A. Marzoughi, R. Burgos, D. Boroyevich, Y. Xue, Design and comparison of cascaded H-BridgeModular multi-level converter, and 5-L active neutral point clamped topologies for motor drive applications, IEEE Trans. Ind. Appl. 54 (2) (2018) 1404–1413.
[17] Z. Zheng, K. Wang, L. Xu, Y. Li, A hybrid cascaded multi-level converter for battery energy management applied in electric vehicles, IEEE Trans. Power Electron. 29 (7) (2014) 3537–3546.
[18] Z. Gao, Q. Lu, A hybrid cascaded multi-level converter based on three-level cells for battery energy management applied in electric vehicles, IEEE Trans. Power Electron. 34 (8) (2019) 7326–7349.
[19] M. Nguyen, T. Tran, Quasi cascaded H-bridge five-level boost inverter, IEEE Trans. Ind. Electron. 64 (11) (2017) 8525–8533.
[20] Z. Du, B. Ozpineci, L.M. Tolbert, J.N. Chiasson, Inductorless DC-AC cascaded H-bridge multi-level boost inverter for electric/hybrid electric vehicle applications, in: IEEE Industry Applications Annual Meeting, IEEE, 2007, pp. 603–608.
[21] J. Wu, J. Ruan, N. Zhang, P.D. Walker, Optimized real-time energy management strategy for the power-split hybrid electric vehicles, IEEE Trans. Control Syst. Technol. 27 (3) (2019) 1194–1202.
[22] A. Ghazanfari, A.I. MohamedY, A resilient framework for faultfault-tolerant operation of modular multi-level converters, IEEE Trans. Ind. Electron. 63 (5) (2016) 2669–2678.
[23] Y. Li, K. Li, Incorporating demand response of electric vehicles in scheduling of isolated microgrids with renewables using a Bi-level programming approach, IEEE Access 7 (2019) 116256–116266.
[24] Y. Zhang, X. Cheng, C. Yin, S. Cheng, A soft-switching bidirectional DC–DC converter for the battery super-capacitor hybrid energy storage system, IEEE Trans. Ind. Electron. 65 (10) (2018) 7856–7865.
[25] X. Peng, X. He, P. Han, et al., Opposite vector based phase shift carrier space vector pulse width modulation for extending the voltage balance region in single-phase 3LNPC cascaded rectifier, IEEE Trans. Power Electron. 32 (9) (2017) 7381–7393.
[26] H. Wang, J. Cao, Z. He, et al., Research on overvoltage for XLPE cable in a modular multi-level converter HVDC transmission system, IEEE Trans. Power Deliv. 31 (2) (2016) 683–692.
[27] L. Harnefors, N. Johansson, L. Zhang, Impact on interarea modes of fast HVDC primary frequency control, IEEE Trans. Power Syst. 32 (2) (2017) 1350–1358.
[28] A Elserougi Ahmed, M Massoud Ahmed, Shehab Ahmed, A switched-capacitor submodule for modular multi-level HVDC converters with DC-fault blocking capability and a reduced number of sensors, IEEE Trans. Power Deliv. 31 (2) (2016) 762, 762.
[29] F. Li, F. He, Z. Ye, et al., A simplified PWM strategy for three-level converters on three-phase four-wire active power filter, IEEE Trans. Power Electron. 33 (5) (2018) 4396–4406.
[30] M.A. Azzouz, A. Hooshyar, Dual current control of inverter-interfaced renewable energy sources for precise phase selection, IEEE Trans. Smart Grid 10 (5) (2019) 5092–5102.
[31] M. Huang, Y. Peng, C.K. Tse, et al., Bifurcation and large-signal stability analysis of three-phase voltage source converter under grid voltage dips, IEEE Trans. Power Electron. 32 (11) (2017) 8868–8879.
[32] N. Thitichaiworakorn, M. Hagiwara, H. Akagi, A medium-voltage large wind turbine generation system using an AC/AC modular multi-level cascade converter, IEEE Journal of Emerging and Selected Topics in Power Electronics 4 (2) (2016) 534–546.
[33] A. Sivapriya, N. Kalaiarasi, A novel enhanced deep learning-based fault diagnosis approach for cascaded multilevel inverter, e-Prime - advances in Electrical Engineering, in: Electronics and Energy, vol. 5, 2023 100253, https://doi.org/10.1016/j.prime.2023.100253. ISSN 2772-6711.
[34] A. Sivapriya, N. Kalaiarasi, R. Verma, B. Chokkalingam, J.L. Munda, Fault diagnosis of cascaded multilevel inverter using multiscale kernel convolutional neural network, IEEE Access 11 (2023) 79513–79530, https://doi.org/10.1109/ACCESS.2023.3299852.
[35] B. Du, Y. He, C. Zhang, Intelligent diagnosis of cascaded H-bridge multilevel inverter combining sparse representation and deep convolutional neural networks, IET Power Electron. 14 (6) (2023) 1121–1137, https://doi.org/10.1049/pel2.12094.
[36] N. Raj, G. Jagadanand, S. George, Fault detection and diagnosis in asymmetric multilevel inverter using artificial neural network, Int. J. Electron. 105 (4) (2018) 559–571, https://doi.org/10.1080/00207217.2017.1378382.
[37] T.Z. Wang, J. Qi, H. Xu, Y.D. Wang, L. Liu, D.J. Gao, Fault diagnosis method based on FFT-RPCA-SVM for Cascaded-Multilevel Inverter, ISA Trans. 60 (2016) 156–163, https://doi.org/10.1016/j.isatra.2015.11.018.
[38] Q. Yuan, Q. Tu, L. Yan, K. Xia, Fault diagnosis of H-bridge cascaded five-level inverter based on improved support vector machine with gray wolf algorithm, Energy Rep. 9 (2023) 485–495, https://doi.org/10.1016/j.egyr.2023.03.017.
[39] Murad Ali, Zakiud Din, Evgeny Solomin, Khalid Mehmood Cheema, Ahmad H. Milyani, Zhiyuan Che, Open switch fault diagnosis of cascade H-bridge multi-level inverter in distributed power generators by machine learning algorithms, Energy Rep. 7 (2021) 8929–8942, https://doi.org/10.1016/j.egyr.2021.11.058.
[40] Rinsha, V., & Jagadanand, G., "Rolling Average-Decision Tree-Based Fault Detection of Neutral Point Clamped Inverters", IEEE Journal of Emerging and Selected Topics in Industrial Electronics, vol. 4, no. 3, pp. 744-755. https://doi.org/10.1109/JESTIE.2023.3236587.
[41] E. Parimalasundar, S. Jayakumar, Sudha Dukkipati, S. Sudha, S. Sivarajan, B. Hemanth Kumar, A novel approach to fault recognition in multi-level inverters through artificial neural networks, SSRG International Journal of Electrical and Electronics Engineering 11 (5) (May 2024) 161–174. ISSN: 2348-8379/.
[42] M. Hoyerby, J.K. Jakobsen, J. Midtgaard, T.H. Hansen, A 70MW monolithic five-level class-D audio power amplifier in 180nm BCD, IEEE J. Solid State Circ. 51 (12) (2016) 2819–2829.
[43] I. Sarkar, B.G. Fernandes, Fault-tolerant operation of nine-level hybrid symmetric cascaded multi-level converter[C]. National Power Electronics Conference, IEEE, 2017, pp. 191–196.
[44] Y. Lien, E.A.M. Klumperink, B. Tenbroek, et al., Enhanced-selectivity high-linearity low-noise mixer-first receiver with complex Pole pair due to capacitive positive feedback, IEEE J. Solid State Circ. 53 (5) (2018) 1348–1360.
[45] N. Seth, V. Goel, R.D. Kulkarni, V.P. Joshi, Performance analysis of seven level three phase asymmetric multi-level inverter at various modulation indices[C], International Conference on Electrical Power and Energy Systems. IEEE (2016) 407–413.
[46] X. Su, H. Liu, Y. Fu, P. Wolfs, Multi-objective DSTATCOM placement based on sensitivity analysis and genetic algorithm in unbalanced MV distribution networks[C]//IEEE innovative smart grid technologies, IEEE (2017) 1–5.
[47] Torricelli G. PastorelliA, M. Scabia, et al., A real-time 2-D vector Doppler system for clinical experimentation, IEEE Trans. Med. Imag. 27 (10) (2008) 1515–1524.

[48] C. Xu, K. Dai, X. Chen, Y. Kang, Voltage droop control at point of common coupling with arm current and capacitor voltage analysis for distribution static synchronous compensator based on modular multi-level converter, IET Power Electron. 9 (8) (2016) 1643–1653.
[49] P. Flores, J. Dixon, M. Ortuzar, et al., Static var compensator and active power filter with power injection capability, using 27-level inverters and photovoltaic cells, IEEE Trans. Ind. Electron. 56 (1) (2009) 130–138.
[50] Y. Liu, F.L. Luo, Trinary hybrid multi-level inverter used in STATCOM with unbalanced voltages[J]. IEE proceedings - electric power applications, IET 152 (5) (2005) 1203–1222.
[51] C. Lee, B. Wang, S. Chen, et al., Average power balancing control of a STATCOM based on the cascaded H-bridge PWM converter with star configuration, IEEE Trans. Ind. Appl. 50 (6) (2014) 3893–3901.
[52] D. Zhou, S. Yang, Y. Tang, Integrating phase-shifted pulse-width modulation to model predictive current control of modular multi-level converters[C]//energy conversion congress and exposition, IEEE (2018) 4845–4850.
[53] R. Gupta, A. Ghosh, A. Joshi, Multiband hysteresis modulation and switching characterization for sliding-mode-controlled cascaded multi-level inverter, IEEE Trans. Ind. Electron. 57 (7) (2010) 2344–2353.
[54] A. Lopez-de-Heredia, H. Gaztañaga, U. Viscarret, et al., Comparison of H-NPC and parallel-H topologies for AC traction front-end converters[C]//European conference on power electronics and applications, IEEE (2009) 1–9.
[55] A. Kumar, H. BhatA, P. Agarwal, Comparative analysis of dual active bridge isolated DC to DC converter with flyback converters for bidirectional energy transfer[C]//recent developments in control, automation & power engineering, IEEE (2017) 382–387.
[56] R. Thekkeppat, V. Mandloi, P. Shrivastava, A solid-state converter topology100 kV, 20 A, 1.6 ms, modulator for high average power klystron amplifier, IEEE Trans. Plasma Sci. 46 (10) (2018) 3700–3707.
[57] V. Waghamare, A.S. Salvi, Industrial purposed advance controlling strategy for SVC compensator firing system using microprocessor[C]//international conference for convergence in technology, IEEE (2017) 686–689.
[58] R. Brezovnik, J. Cernelic, M. Petrun, et al., Impact of the switching frequency on the welding current of a spot-welding system, IEEE Trans. Ind. Electron. 64 (12) (2017) 9291–9301.
[59] P. Li, G.P. Adam, D. Holliday, et al., Simulation study of FACTS devices based on AC–AC modular multi-level hexagonal chopper, IET Power Electron. 10 (8) (2017) 919–930.
[60] K. Shen, S. Wang, D. Zhao, G. Zhao, A discrete-time low-frequency-ratio nearest level modulation strategy for modular multi-level converters with small number of power modules, IEEE Access 7 (2019) 25792–25803.
[61] D. Ronanki, S.S. Williamson, Modular multi-level converters for transportation electrification: challenges and opportunities, IEEE Transactions on Transportation Electrification 4 (2) (2018) 399–407.
[62] S. Dieckerhoff, S. Bernet, D. Krug, Power loss-oriented evaluation of high voltage IGBTand multi-level converters in transformerless traction applications, IEEE Trans. Power Electron. 20 (6) (2005) 1328–1336.
[63] J. Dixon, L. Moran, A clean four-quadrant sinusoidal power rectifier using multistage converters for subway applications, IEEE Trans. Ind. Electron. 52 (3) (2005) 653–661.
[64] T.A. Meynard, H. Foch, P. Thomas, et al., Multicell converters: basic concepts and industry applications, IEEE Trans. Ind. Electron. 49 (5) (2002) 955–964.
[65] S. Ziaeinejad, A. Mehrizi-Sani, PWM A-CHB converter based on trinary multi-level converter: topology, switching algorithm, and stability analysis, IEEE Trans. Ind. Electron. 66 (6) (2019) 4166–4176.
[66] S. Busquets-Monge, J. Rocabert, P. Rodriguez, et al., Multi-level diode-clamped converter for photovoltaic generators with independent voltage control of each solar array, IEEE Trans. Ind. Electron. 55 (7) (2008) 2713–2723.
[67] D. Alexander, Hybrid electric drive for naval combatants, IEEE 103 (12) (2015) 2267–2275.
[68] U. Javaid, F.D. Freijedo, D. Dujic, W.V.D. Merwe, MVDC supply technologies for marine electrical distribution systems, CPSS Transactions on Power Electronics and Applications 3 (1) (2018) 65–76.
[69] S. Bifaretti, P. Zanchetta, A. Watson, et al., Advanced power electronic conversion and control system for universal and flexible power management, IEEE Trans. Smart Grid 2 (2) (2011) 231–243.
[70] S.K. Chattopadhyay, C. Chakraborty, A new asymmetric multi-level inverter topology suitable for solar PV applications with varying irradiance, IEEE Trans. Sustain. Energy 8 (4) (2017) 1496–1506.
[71] X. Wang, D. Gunasekaran, A. Taylor, et al., Comprehensive design and control of electric powertrain evaluation platform for next generation EV/HEV development, in: IEEE Transportation Electrification Conference and Expo, IEEE, 2018, pp. 237–242.
[72] J. Rodriguez, J. Pontt, G. Alzarnora, et al., Novel 20-MW downhill conveyor system using three-level converters, IEEE Trans. Ind. Electron. 49 (5) (2002) 1093–1100.
[73] D. Gray, Review of marine AC installations [B]//the institution of electrical engineers, Springer Nature 111 (2) (2015) 361–370.
[74] J. Yong, X. Li, W. Xu, Interharmonic source model for current-source inverter-fed variable frequency drive, IEEE Trans. Power Deliv. 32 (2) (2017) 812–821.
[75] Y. Wang, J. Xu, L. Feng, C. Wang, A novel hybrid modular three-level shunt active power filter, IEEE Trans. Power Electron. 33 (9) (2018) 7591–7600.
[76] L. Feng, Y. Wang, Modeling and resonance control of modular three-level shunt active power filter, IEEE Trans. Ind. Electron. 64 (9) (2017) 7478–7486.
[77] H. Salimian, H. Iman-Eini, Fault-tolerant operation of three-phase cascaded H-bridge converters using an auxiliary module, IEEE Trans. Ind. Electron. 64 (2) (2017) 1018–1027.
[78] M. Adly, K. Strunz, Irradiance-adaptive PV module integrated converter for high efficiency and power quality in standalone and DC microgrid applications, IEEE Trans. Ind. Electron. 65 (1) (2018) 436–446.
[79] F. Peng, J. Ye, A. Emadi, An asymmetric three-level neutral point diode clamped converter for switched reluctance motor drives, IEEE Trans. Power Electron. 32 (11) (2017) 8618–8631.
[80] J. Chen, Y. Li, P. Wang, et al., A closed-loop selective harmonic compensation with capacitor voltage balancing control of cascaded multi-level inverter for high-power active power filters[C]. IEEE Power Electronics Specialists Conference, IEEE, 2008, pp. 569–573.
[81] B.J. Kumar, A. Chandramouli, Modeling and simulation of nine-level cascaded H-bridge inverter based shunt active power filter for single-phase distribution system[C]. International Conference on Inventive Computing and Informatics, IEEE, 2017, pp. 675–680.
[82] M. Norambuena, C. Garcia, J. Rodriguez, P. Lezana, Finite control set model predictive control reduced computational cost applied to a flying capacitor converter[C]. Annual Conference of the, IEEE Industrial Electronics Society, IEEE, 2017, pp. 4903–4907.
[83] S. Ray, N. Gupta, R.A. Gupta, Advanced PWMfor balancing DC-link voltages in seven-level CHB inverter based active filter[C]//recent developments in control. Automation & Power Engineering, IEEE, 2017, pp. 291–296.
[84] Z. Shu, S. Xie, Q. Li, Single-phase back-to-back converter for active power balancing, reactive power compensation, and harmonic filtering in traction power system, IEEE Trans. Power Electron. 26 (2) (2011) 334–343.
[85] H.A. Zebker, User-friendly inSAR data products: fast and simple timeseries processing, Geosci. Rem. Sens. Lett. IEEE 14 (11) (2017) 2122–2126.
[86] M. Chen, B. Zhang, Y. Li, et al., Design of A Multi-Level battery management system for A cascade H-bridge energy storage system. C]//PES Asia-Pacific Power and Energy Engineering Conference, IEEE, 2014, pp. 1–5.
[87] S. Cailhol, P. Vidal, F. Rotella, A generic method of pulsewidth modulation applied to three-phase three-level T-type NPC inverter, IEEE Trans. Ind. Appl. 54 (5) (2018) 4515–4522.
[88] E. Afshari, G.R. Moradi, R. Rahimi, et al., Control strategy for three-phase grid-connected PV inverters enabling current limitation under unbalanced faults, IEEE Trans. Ind. Electron. 64 (11) (2017) 8908–8918.
[89] Z. PengF, Y. Liu, S. Yang, et al., Transformer-less unified power-flow controller using the cascade multi-level inverter, IEEE Trans. Power Electron. 31 (8) (2016) 5461–5472.
[90] S. Kim, H. Kim, H. Cha, Dynamic voltage restorer using switching cell structured multi-level AC–AC converter, IEEE Trans. Power Electron. 32 (11) (2017) 8406–8418.

[91] M. Pradhan, M.K. Mishra, Dual P-Q theory based energy-optimized dynamic voltage restorer for power quality improvement in a distribution system, IEEE Trans. Ind. Electron. 66 (4) (2019) 2946–2955.
[92] A. Joseph, K. Desingu, R.R. Semwal, et al., Dynamic performance of pumping mode of 250 MW variable speed hydro-generating unit subjected to power and control circuit faults, IEEE Trans. Energy Convers. 33 (1) (2018) 430–441.
[93] P. MiniV, N. Mayadevi, R. Hari Kumar, S. Ushakumari, A novel algorithm for detection and diagnosis of switching faults of three phase induction motor drive system, in: International Conference on Power Electronics, Drives and Energy Systems, IEEE, 2018, pp. 1–4.
[94] Q. An, L. Sun, K. Zhao, L. Sun, Switching function model-based fast-diagnostic method of open-switch faults in inverters without sensors, IEEE Trans. Power Electron. 26 (1) (2011) 119–126.
[95] E. Pons, R. Tommasini, P. Colella, Fault current detection and dangerous voltages in DC urban rail traction systems, IEEE Trans. Ind. Appl. 53 (4) (2017) 4109–4115.
[96] H. Lee, A. Lee, S. Wang, et al., Analysis and compact modeling of magnetic tunnel junctions utilizing voltage-controlled magnetic anisotropy, IEEE Trans. Magn. 54 (4) (2018) 1–9.
[97] W. Chen, X. Fu, C. Xue, et al., Indirect input-series output-parallel DC–DC full bridge converter system based on asymmetric pulsewidth modulation control strategy, IEEE Trans. Power Electron. 34 (4) (2019) 3164–3177.
[98] Y. Son, J. Ha, Direct power control of a three-phase inverter for grid input current shaping of a single-phase diode rectifier with a small DC-link capacitor, IEEE Trans. Power Electron. 30 (7) (2015) 3794–3803.
[99] M.A. Rodriguez-Blanco, A. Claudio-Sanchez, D. Theilliol, et al., A failure-detection strategy for IGBT based on gate-voltage behavior applied to a motor drive system, IEEE Trans. Ind. Electron. 58 (5) (2011) 1625–1633.
[100] L. Zipeng, L. Jinjun, L. Zeng, et al., The optimization analysis of impulse injection method for impedance measurement in three-phase power electronic systems [C], in: International Future Energy Electronics Conference and ECCE Asia, IEEE, 2017, pp. 1623–1627.
[101] Godoy S. Marcelo, A.F. Felix, Digital processing techniques applied to power electronics. In modeling power electronics and interfacing energy conversion systems, IEEE Access 1 (5) (2017) 279–320.
[102] B. Wen, R. Burgos, D. Boroyevich, et al., AC stability analysis and DQFrame impedance specifications in power-electronics-based distributed power systems, IEEE Journal of Emerging and Selected Topics in Power Electronics 5 (4) (2017) 1455–1465.
[103] J. Ge, Z. Zhao, L. Yuan, et al., Direct power control based on natural switching surface for three-phase PWM rectifiers, IEEE Trans. Power Electron. 30 (6) (2015) 2918–2922.
[104] C. Verdugo, J.I. Candela, F. Blaabjerg, P. Rodriguez, Three-phase isolated multi-modular converter in renewable energy distribution systems, IEEE Journal of Emerging and Selected Topics in Power Electronics 1 (5) (2019) 1–6.
[105] K. Ali, R.K. Surapaneni, P. Das, S.K. Panda, An SiC-MOSFET-Based nine-switch single-stage three-phase AC-DC isolated converter, IEEE Trans. Ind. Electron. 64 (11) (2017) 9083–9093.
[106] Z. Gao, C. Cecati, S.X. Ding, A survey of fault diagnosis and faultfault-tolerant techniquesPart I: fault Diagnosis with model-based and signal-based approaches, IEEE Trans. Ind. Electron. 62 (6) (2015) 3757–3767.
[107] Y. Chen, B. Hou, Z. He, J. Wang, General process model for unanticipated fault diagnosis of complex system based on data driven, Natlional University Defense Technology 39 (6) (2017) 126–133.
[108] Y. Liu, L. Ma, S. Huang, Fault diagnosis and isolation process of gas turbine based on Fault dependency, in: International Conference on Computational Intelligence and Natural Computing, IEEE, 2009, pp. 441–444.
[109] Y. Du, X. Pang, Z. Yang, Fault diagnosis method of shear gearbox[pattent], Ind. Mine Autom. 43 (12) (2017) 95–98.
[110] W. Ziling, X. Aiqiang, Y. Zhiyong, Application of model-based and data-driven techniques in fault diagnosis, in: International Conference on Electronic Measurement and Instruments, IEEE, 2007, pp. 451–454.
[111] h Jiang, S. Yang, Modeling method for information model of fault tree diagnosis based on UML, in: International Conference on Computer Science and Information Technology, IEEE, 2010, pp. 238–241.
[112] Q. Hu, A. Qin, Q. Zhang, et al., Fault diagnosis based on weighted extreme learning machine with wavelet packet decomposition and KPCA, IEEE Sensor. J. 18 (20) (2018) 8472–8483.
[113] M. Sohaib, C.H. Kim, J.M. Kim, A hybrid feature model and deep-learning-based bearing fault diagnosis, Sensors 17 (12) (2017) 1–9.
[114] Kumar S. Tapan, P. Prithwiraj, Smart transformer condition monitoring and diagnosis, In Transformer Ageing: Monitoring and Estimation Techniques 5 (56) (2017) 89–95. IEEE Aceess.
[115] R. Costa-Castello, V. Puig, J. Blesa, On teaching model-based fault diagnosis in engineering curricula [L], IEEE Control Syst. Mag. 36 (1) (2016) 53–62.
[116] G. Provan, C. Yi-Liang, Model-based fault-tolerant control reconfiguration for general network topologies, IEEE Microelectronics 21 (5) (2001) 64–76.
[117] C.H. Zhao, W.Q. Li, Y.X. Sun, F.R. Gao, Multiple local reconstruction model-based fault diagnosis for continuous processes, Zidonghua Xuebao/Acta Automatica Sinica 39 (5) (2013) 487–493.
[118] R.R. Soman, E.M. Davidson, S.D.J. Mcarthur, et al., Model-based methodology using modified sneak circuit analysis for power electronic converter fault diagnosis, IET Power Electron. 5 (6) (2012) 813–826.
[119] K. Hu, Z. Liu, K. Huang, et al., Improved differential evolution algorithm of model-based diagnosis in traction substation fault diagnosis of high-speed railway, IET Electr. Syst. Transp. 6 (3) (2016) 163–169.
[120] Y.Y. Wang, Y. Sun, C.F. Chang, Y. Hu, Model-based Fault Detection and faultfault-tolerant control of SCR urea injection systems, IEEE Trans. Veh. Technol. 65 (6) (2016) 4645–4654.
[121] J. Cui, Q. Zheng, Y. Xin, et al., Feature extraction and classification method for switchgear faults based on sample entropy and cloud model, IET Gener. Transm. Distrib. 11 (11) (2017) 2938–2946.
[122] D.R. Espinoza-Trejo, D.U. Campos-Delgado, E. Barcenas, et al., Fault diagnosis scheme for open-circuit FaultsiIn voltage source inverters feeding induction motors by using nonlinear proportional-integral observers, IET Power Electron. 5 (7) (2012) 1204–1216.
[123] D. Henry, C.L. Peuvedic, L. Strippoli, F. Ankersen, Robust model-based fault diagnosis of thruster faults in spacecraft, IFAC-PapersOnLine 48 (21) (2015) 1078–1083.
[124] Z. Liao, P. Chen, A vibration signal filtering method based on KL divergence genetic algorithm with application to low speed bearing fault diagnosis[C]. International Conference on Digital Signal Processing. IEEE, 2018, pp. 1–5.
[125] C.Q. Shen, J.Q. Xie, D. Wang, et al., Improved hierarchical adaptive deep belief network for bearing fault diagnosis, Applied Sciences-Basel 9 (16) (2019) 53–60.
[126] S. Choi, B. Akin, M.M. Rahimian, H.A. Toliyat, Implementation of a Fault-diagnosis algorithm for induction machines based on advanced digital-signal-processing techniques, IEEE Trans. Ind. Electron. 58 (3) (2011) 937–948.
[127] Nie Y, Zhao Y, Li H. Bearing Fault Identification Method, Involves Analyzing Vibration Signal to Obtain Fault Type According to Characteristic Frequency, and Performing Bearing Fault Judging Process by Utilizing Analyzed Vibration Signal [Pattent]. CN110057583-A.
[128] Baddour N. HuangH, M. Liang, A method for tachometer-free and resampling-free bearing fault diagnostics under time-varying speed ConditionMeasurement, Journal of the International Measurement Confederation 134 (2019) 101–117.
[129] P. Chao-yong, W. Ai, P. Jian-ping, G. Xiao-rong, Wayside acoustic diagnosis of axle box bearing based on fault feature extraction algorithm[C]//far east NDT new technology & application forum, IEEE (2018) 90–94.
[130] C.Y. Yang, T.Y. Wu, Diagnostics of gear deterioration using EEMD approach and PCA process, Journal of the International Measurement Confederation 61 (2015) 75–87.
[131] Henry P S, Gerszberg I. Method for Detecting Fault in Communication System, Involves Determining whether Set of Antenna Systems Experience Operational Fault from Frequency Domain Comparison Information of Returned Message by First Antenna System[P]//US2019268079-A1.

[132] Z. Liu, Z. Jia, C. Vong, et al., Capturing high-discriminative fault features for electronics-rich analog system via deep learning, IEEE Trans. Ind. Inf. 13 (3) (2017) 1213–1226.
[133] Y. Xin, S.M. Li, Novel data-driven short-frequency mutual information entropy threshold filtering and its application to bearing fault diagnosis, Meas. Sci. Technol. 30 (11) (2019) 12–20.
[134] M.I. Zaki, R.A. El-Sehiemy, G.M. Amer, et al., An investigated reactive power measurements-based fault-identification scheme for teed transmission lines, Journal of the International Measurement Confederation 136 (2019) 185–200.
[135] D. Tzelepis, A. Dyko, G. Fusiek, et al., Advanced Fault location in MTDC networks utilising optically-multiplexed current measurements and machine learning approach, Int. J. Electr. Power Energy Syst. 97 (2018) 319–333.
[136] Z. Nan, Mechanical Fault diagnosis method based on machine learning, in: International Conference on Measuring Technology and Mechatronics Automation, IEEE, 2015, pp. 626–629.
[137] C.G. Dias, C.M. DeSousa, A neuro-fuzzy approach for locating broken rotor bars in induction motors at very low slip, Journal of Control, Automation and Electrical Systems 29 (4) (2018) 489–499.
[138] G. Yuan, D. Liu, S. Liang, et al., Fault diagnosis of VNA intermediate frequency processing system based on dynamic fuzzy neural network[C]. International Conference on Communication Technology, IEEE, 2015, pp. 192–195.
[139] J.Y. Dai, J. Tang, F.M. Shao, et al., Fault diagnosis of rolling bearing based on multiscale intrinsic mode function permutation entropy and a stacked sparse denoising autoencoder, Applied Sciences-Basel 9 (13) (2019) 81–89.
[140] A. Haque, K.V.S. Bharath, M.A. Khan, et al., Fault diagnosis of photovoltaic modules, Energy Sci. Eng. 7 (3) (2019) 622–644.
[141] C. Yong, H. Yihuai, Fault diagnosis of marine diesel engine based on blind source separation[C], International Conference on Computer and Automation Engineering. IEEE (2010) 1–3.
[142] J. Pan, Y.Y. Zi, J.L. Chen, et al., A novel deep learning network with layerwise feature learning from noisy mechanical data for fault classification, IEEE Trans. Ind. Electron. 65 (6) (2018) 4973–4982.
[143] M. Askarian, G. Escudero, M. Graells, et al., Fault diagnosis of chemical processes with incomplete observations: a comparative study [B], Comput. Chem. Eng. 84 (2016) 104–116.
[144] P. Colombo, Closed Loop Controlled Electronic Carburation System, P]//SAE International, 2010.
[145] M. Darabian, A. Jalilvand, M. Azari, Power system stability enhancement in the presence of renewable energy Resources and HVDC lines based on predictive control strategy, Int. J. Electr. Power Energy Syst. 80 (2016) 363–373.
[146] Cheng L. ZhaoH, Open-circuit faults diagnosis in back-to-back converters of DF wind turbine, IET Renew. Power Gener. 11 (4) (2017) 417–424.
[147] A. Khoshnami, I. Sadeghkhani, Sample entropy-based Fault Detection for photovoltaic arrays, IET Renew. Power Gener. 12 (16) (2018) 1966–1976.
[148] R.C. Thomson, G.P. Harrison, J.P. Chick, Marginal greenhouse GAS emissions displacement of wind power in great britain[P], Energy Pol. 101 (2017) 201–210.
[149] F. Cheng, J. Wang, L. Qu, W. Qiao, Rotor-current-based fault diagnosis for DFIG wind turbine drivetrain gearboxes using frequency analysis and a deep classifier, IEEE Trans. Ind. Appl. 54 (2) (2018) 1062–1071.
[150] S.H. Kia, H. Henao, G. Capolino, Fault index statistical study for gear Fault detection using stator current space vector analysis, IEEE Trans. Ind. Appl. 52 (6) (2016) 4781–4788.
[151] G. Ivensky, M. Gulko, S. Ben-Yaarov, Current-Fed multiresonant isolated DC-DC converter, IEEE Trans. Aero. Electron. Syst. 33 (1) (1997) 53–63.
[152] R.T. Yanushevsky, Optimal strategic planning problems in manufacturing based on the input-output models, Appl. Math. Model. 16 (4) (1992) 208–213.
[153] M. Mishra, P. Routray, P.K. Rout, A universal high impedance Fault Detection technique for distribution system using S-transform and, Pattern Recognition [P]//Technology Economic Smart Grids SustainEnergy 1 (1) (2016) 9–14.
[154] Y. Maouche, M.E.K. Oumaamar, M. Boucherma, A. Khezzar, Instantaneous power spectrum analysis for broken bar Fault Detection in inverter-fed six-phase squirrel cage induction motor, Int. J. Electr. Power Energy Syst. 62 (2014) 110–117.
[155] F.M. Modesto, M.F. Caetano, J.L. Bordim, A dynamic spectrum access MAC protocol based on spectrum analysis and spectrum sharing[C]//Conferencia latinoamericana en informatica, Springer Nature (2012) 1–8.
[156] Q.B. Tong, J.C. Cao, B.Z. Han, et al., A Fault diagnosis approach for rolling element bearings based on dual-tree complex wavelet packet transform-improved intrinsic time-scale decomposition, singular value decomposition, and online sequential extreme learning machine, Adv. Mech. Eng. 9 (12) (2017) 1958–1969.
[157] W. Jun, X. Jian, H. Dan, Fuzzy wavelet network modeling with B-spline wavelet[C], in: International Conference on Machine Learning and Cybernetics, IEEE, 2005, pp. 4144–4148.
[158] Z. Yang, X. Li, C. Zhang, S. Chi, A new slip compensation method for induction motors based on current vector decoupling, in: International Conference on Electrical Machines and Systems, IEEE, 2017, pp. 1–6.
[159] M. Schlechtingen, I.F. Santos, S. Achiche, Using data-mining approaches for wind turbine power curve monitoring, IEEE Trans. Sustain. Energy 4 (3) (2013) 671–679.
[160] Z.P. Feng, X.W. Chen, M. Liang, Iterative generalized synchrosqueezing transform for fault diagnosis of wind turbine planetary gearbox under nonstationary conditions, Mech. Syst. Signal Process. 6 (74) (2015) 52–53.
[161] Z. Feng, X. Song, F. Chu, Fault diagnosis based on integration of cluster analysis, rough set method and fuzzy neural network, Chin. J. Mech. Eng. 17 (3) (2004) 349–352.
[162] J.W. Forrester, Applications of Bond Graphs to Modelling Industrial Processes and Manufacturing Systems[C]//IEE Colloquium on Bond Graphs in Control, IET, 1990, pp. 1–8.
[163] Luis RT. Jose, G.L. Francisco, Pattern Recognition-Based Approach for Dynamic Vulnerability Status Prediction in Dynamic Vulnerability Assessment and Intelligent Control[C]//Sustainable Power Systems, IEEE, 2018, pp. 95–117.
[164] R.E. Locher, Short circuit proof IGBTs simplify overcurrent protection[C]//industry applications society annual meeting, IEEE (1991) 1497–1500.
[165] M.S. Jha, G. Dauphin-Tanguy, B. Ould Bouamama, New concept of junction activity in A bond graph model: application for Fault Identification, International Conference on Bond Graph Modeling and Simulation. IEEE (2014) 148–154.
[166] X. Perpina, J.F. Serviere, X. Jorda, et al., IGBT module failure analysis in railway applications, Microelectron. Reliab. 48 (8–9) (2008) 1427–1431.
[167] Y. Hu, Z. Zhu, K. Liu, Current control for dual three-phase permanent magnet synchronous motors accounting for current unbalance and harmonics, IEEE Journal of Emerging and Selected Topics in Power Electronics 2 (2) (2014) 272–284.
[168] M. Cheong, I. Lee, S. Kang, A 3D rotation based through-silicon via redundancy architecture for clustering faults, IEEE Trans. Comput. Aided Des. Integrated Circ. Syst. 5 (56) (2019) 1, 1.
[169] E. Sicard, J. Font, M. Homar, A. Rubio, An integrated approach to real-time pattern recognition, Proceedings[C]//IAPR International Conference on Pattern Recognition. IEEE (1992) 177–180.
[170] A. Sasidharan, P. Palakkeel, Performance of pattern recognition algorithms in identifying banking networks[C]. International Conference on Advances in Computing Communications and Informatics, IEEE, 2018, pp. 1463–1467.
[171] A.R. Abbasi, M.R. Mahmoudi, Z. Avazzadeh, Diagnosis and clustering of power transformer winding fault types by cross-correlation and clustering analysis of FRA results, IET Gener. Transm. Distrib. 12 (19) (2018) 4301–4309.
[172] W.J. Sun, S.Y. Shao, R. Zhao, et al., A sparse auto-encoder-based deep neural network approach for induction motor faults classification, Electrical Measurements 89 (2016) 171–178.
[173] V.S. Thakur, K. Thakur, S. Gupta, K.R. Rao, Improved optimum nonnegative integer bit allocation algorithm using fuzzy domain variance estimation and refinement for the wavelet-based image compression, Circ. Syst. Signal Process. 38 (8) (2019) 3880–3900.
[174] W. Huang, S. Oh, W. Pedrycz, Hybrid fuzzy wavelet neural networks architecture based on polynomial neural networks and fuzzy set/relation inference-based wavelet neurons, IEEE Transact. Neural Networks Learn. Syst. 29 (8) (2018) 3452–3462.
[175] A.L.E. Abreu, A.C. Neto, Machine learning model for predicting evaporation losses in reservoirs, IEEE Latin America Transactions 16 (7) (2018) 2040–2044.

[176] H. Mathkour, A. Al-Salamah, Machine learning technique for monitoring database systems, IEEE Symposium on Computers and Communications. IEEE (1995) 421–427.
[177] B. Du, Y. He, C. Zhang, Intelligent diagnosis of cascaded H-bridge multilevel inverter combining sparse representation and deep convolutional neural networks, IET Power Electron. 14 (6) (2021) 1121–1137, https://doi.org/10.1049/pel2.12094.
[178] F. Jin-Shun, W. Hui, A study of multiple vector-valued wavelet packets associated with A dilation matrix in higher dimensions[C], in: International Conference on Wavelet Analysis and Pattern Recognition, IEEE, 2008, pp. 507–512.
[179] H. Toda, Z. Zhong, Perfectly translation-invariant complex wavelet packet transforms, in: International Conference on Wavelet Analysis and Pattern Recognition, IEEE, 2009, pp. 374–379.
[180] R. Ahmed, P. Srinivasa Pai, N.S. Sriram, V. Bhat, Comparison of wavelet based denoising schemes for gear condition monitoring: an artificial neural network based approach. International Conference on Advances in Materials and Manufacturing Applications.Book Series, 2018, pp. 5–12.
[181] S.M.A. Cruz, A.J.M. Cardoso, Stator winding fault diagnosis in three-phase synchronous and asynchronous motors by the extended Park's vector approach, IEEE Trans. Ind. Appl. 37 (5) (2001) 1227–1233.
[182] A. Sivapriya, N. Kalaiarasi, "A Novel Enhanced Deep Learning-Based Fault Diagnosis Approach for Cascaded Multilevel Inverter. E-Prime-Advances in Electrical Engineering", Electronics and Energy, 2023 100253, https://doi.org/10.1016/j.prime.2023.100253.